5 Post-processing methods for passivity enforcement

Stefano Grivet-Talocia and Luis Miguel Silveira

5 Post-processing methods for passivity enforcement

Abstract: Many physical systems are passive (or dissipative): they are unable to generate energy on their own, but they can store energy in some form while exchanging power with the surrounding environment. This chapter describes the most prominent approaches for ensuring that Reduced Order Models are passive, so that their mathematical representation satisfies an appropriate dissipativity condition. The main focus is on Linear and Time-Invariant (LTI) systems in state-space form. Different conditions for testing passivity of a given LTI model are discussed, including Linear Matrix Inequalities (LMIs), Frequency-Domain Inequalities, and spectral conditions on associated Hamiltonian matrices. Then we describe common approaches for perturbing a given non-passive system to enforce its passivity. Various examples from electronic applications are used to demonstrate both theory and algorithm performance.

Keywords: passivity, dissipativity, positive real lemma, bounded real lemma, Hamiltonian matrices, state-space systems, descriptor systems, eigenvalue perturbation

5.1 Introduction and motivations

Let us consider the problem of designing a complete electronic product, such as a smartphone or a high-end computing server. The complexity of such a system is overwhelming: a single microprocessor might include several billions transistors, and this is just one component. All components are tightly interconnected to exchange signals and power: they interact both through electrical connections as well as (unwanted) electromagnetic couplings, which are inevitable due to the close proximity of components in tightly integrated systems. A proper design flow must ensure that all signals behave as expected during real operation, which requires accounting for all interactions between components and subsystems. A first-pass design can only be achieved by extensive numerical simulation at the system level, in order to verify full compliance with specifications.

All of us would agree that a direct, brute-force simulation of the complete system is totally unrealistic. This is why common engineering practices partition a given complex system into several simpler subsystems, which are modeled independently. All models are then interconnected to obtain a system description that is amenable for numerical simulation. These individual models are very often obtained through

Stefano Grivet-Talocia, Dept. Electronics and Telecommunications, Politecnico di Torino, Turin, Italy
Luis Miguel Silveira, INESC-ID/DEEC, IST Técnico Lisboa, Universidade de Lisboa, Lisbon, Portugal

https://doi.org/10.1515/9783110498967-005

some Model Order Reduction scheme applied to some initial device-level characterization.

Suppose now that one of the above individual models represents some signal or power interconnect network. Such interconnect structure is intended to feed signal and power supply to all elements of the system, in the form of electrical current flowing through metal wires. The interconnect network is unable to generate energy on its own, but rather redistributes the energy that it receives from its input signals to its output signals. It may store energy through electric and magnetic field densities in the physical space surrounding the interconnect, and it may dissipate energy as heat through metal and dielectric losses, but no more energy can be supplied to the environment than the amount of energy previously stored. Such a system is called dissipative (or passive). The concept of dissipativity naturally arises from energy conservation principles and is therefore ubiquitous in several engineering fields.

A (reduced order) model of the interconnect must respect such property: the simulation model must not be able to release more energy than previously stored. This requirement is not just for self-consistency with fundamental physical principles, but for a very practical reason: a non-passive model may trigger instabilities during system-level simulation. An example is provided in Figure 5.1, which compares the voltage received by a state of the art (at the time of writing) smartphone through a high-speed interconnect, computed using a passive vs. non-passive model connected to various other system parts, including drivers and receiver circuits that send and receive the signals. The non-passive model triggers a resonance, by injecting a continuous flow of power that is responsible for the instability. Conversely, the passive model provides a well-behaved bounded response.

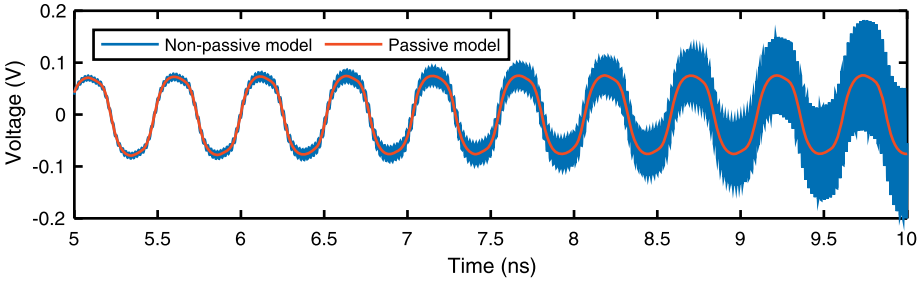

Figure 5.1: Comparison between the responses of passive (thick line) and non-passive (thin line) models of a high-speed smartphone interconnect link.

A fundamental result states that the interconnection of passive subsystems leads to a passive system; see e. g. [74]. Therefore, a guarantee of passivity for all individual

models for which this requirement is adequate[1] is also a guarantee that a model-based system-level simulation will run smoothly. This is a relevant problem not only for electronic applications, but for several applied engineering fields such as, e. g., mechanics or fluid dynamics. Energy conservation or dissipation properties must be preserved in the simulation models.

Figure 5.1 illustrates in a clear manner that any modeling procedure used for analysis of the dynamics of dissipative physical systems should ensure that the resulting model or reduced order model is dissipative. There exist MOR algorithms that are able to preserve dissipativity if applied to an original large-scale dissipative model. Examples are the PRIMA algorithm [63, 67] (see also [6, Chapter 4]) or the PR-TBR algorithm [19, 62, 64, 65, 68] (see also [5, Chapter 2]). Unfortunately, for a variety of reasons, possibly including efficiency considerations, such schemes are not always applicable, and one has to resort to one of the many reduced order modeling techniques that are not able to preserve or enforce dissipativity. Therefore, it is often necessary to perform a-posteriori checks and possibly implement a post-processing procedure that enforces model passivity.

In this Chapter, we review the various forms in which the passivity conditions of a model can be stated. The particular class of systems that we focus on is defined in Section 5.2, although generalizations are discussed in Section 5.6. Different forms of passivity conditions will lead to corresponding different numerical schemes for their verification, discussed in Section 5.3. We then present in Section 5.5 a selection of methods for passivity enforcement, mainly cast as perturbation approaches that, starting from the original non-passive model, update its coefficients in order to achieve passivity. Model accuracy is retained by minimizing the perturbation amount in some norm, as discussed in Section 5.4.

The style of this chapter is informal, with main results being stated with some essential derivation, but without a formal proof. Emphasis is on the practical aspects of the various formulations, which lead to algorithms presented in pseudocode form. Pointers to the relevant literature are provided for additional insight.

5.2 Passivity conditions

In order to keep this chapter self-contained, our discussion is based on the special class of Linear Time-Invariant (LTI), finite-dimensional systems in regular state-space form

$$\mathcal{S}: \quad \begin{cases} \dot{x}(t) = Ax(t) + Bu(t), \\ y(t) = Cx(t) + Du(t), \end{cases} \tag{5.1}$$

1 Note that not all components are passive: for instance, signal or power sources or amplifier circuits do not and must not be expected to behave as passive elements.

where t denotes time, vectors $u \in \mathcal{U} \subseteq \mathbb{R}^M$ and $y \in \mathcal{Y} \subseteq \mathbb{R}^M$ collect the system inputs and outputs, respectively, and $x \in \mathcal{X} \subseteq \mathbb{R}^N$ is the state vector, with $\dot{x}$ denoting its time derivative. The $M \times M$ transfer function of the system is

$$H(s) = C(sI - A)^{-1}B + D, \tag{5.2}$$

where s is the Laplace variable. We start by assuming the system to be asymptotically stable, with all eigenvalues of A, i. e., the poles of $H(s)$, having a strictly negative real part.

The above assumptions may seem overly restrictive, but most common macromodeling schemes that are widespread in electronic applications such, e. g. the Vector Fitting algorithm [5, Chapter 8], produce reduced order models in this form. Generalizations will be discussed in Section 5.6.

5.2.1 Dissipative systems

The system $\mathcal{S}$ in (5.1) is *dissipative* [15, 74, 88] with respect to the supply function $\mathsf{s} : \mathcal{U} \times \mathcal{Y} \mapsto \mathbb{R}$ if there exists a *storage function* $V : \mathcal{X} \mapsto \mathbb{R}$ such that

$$V(x(t_1)) \leq V(x(t_0)) + \int_{t_0}^{t_1} \mathsf{s}(u(t), y(t))\, dt \tag{5.3}$$

for all $t_0 \leq t_1$ and all input, state and output signals u, x, y that satisfy the state-space equations (5.1). In the above definition, V represents the internal energy that the system is able to store, and s is the power flow exchanged by the system with the environment. Thus, for a dissipative system the increase in the internal energy that the system undergoes during any time interval (t_0, t_1) cannot exceed the cumulative amount of energy received from the environment, expressed as a time integral of the input power flow. If the storage function is differentiable, the *dissipation inequality* (5.3) can also be cast in the equivalent form

$$\frac{dV(x(t))}{dt} \leq \mathsf{s}(u(t), y(t)). \tag{5.4}$$

As a typical example, one may consider an electric RLC circuit made of an arbitrary number of arbitrarily connected resistors $R_k > 0$, inductors $L_k > 0$ and capacitors $C_k > 0$, which interacts with the environment through M ports. Each port defines an input, e. g., the port voltage v_j, with the port current i_j acting as the corresponding output (this representation is called *admittance*). For this example, the state vector comprises all capacitor voltages v_{Ck} and inductor currents i_{Lk}, so that the energy storage function is defined as $V := \frac{1}{2}(\sum_k C_k v_{Ck}^2 + \sum_k L_k i_{Lk}^2)$. The electric power entering the circuit at the jth port is $v_j i_j$, so that the power supply function reads $\mathsf{s}(u, y) = u^T y = \sum_j v_j i_j$.

By Tellegen's (power conservation) theorem [4, 24], we have

$$\begin{aligned}\mathsf{s}(u,y) &= \sum_j v_j i_j = \sum_k v_{Ck} i_{Ck} + \sum_k v_{Lk} i_{Lk} + \sum_k R_k i_{Rk}^2 \\ &= \frac{dV}{dt} + \sum_k R_k i_{Rk}^2 \geq \frac{dV}{dt}\end{aligned} \tag{5.5}$$

where we used the definition of capacitor currents $i_{Ck} = C_k \frac{dv_{Ck}}{dt}$, inductor voltages $v_{Lk} = L_k \frac{di_{Lk}}{dt}$, and where i_{Rk} are the resistor currents. So, we see that any RLC circuit with positive elements is dissipative.

The system $\mathcal{S}$ in (5.1) is called *strictly dissipative* [74, 88] with respect to the supply function s if the stronger condition

$$V(x(t_1)) \leq V(x(t_0)) + \int_{t_0}^{t_1} \mathsf{s}(u(t), y(t))\, dt - \varepsilon^2 \int_{t_0}^{t_1} \|u(t)\|^2\, dt \tag{5.6}$$

holds for some $\varepsilon > 0$ instead of (5.3), which is thus satisfied with a strict inequality.

The following three subsections provide different equivalent passivity conditions that are applicable to linear state-space systems in the form (5.1).

5.2.1.1 Linear matrix inequalities

Building on the above example, we consider for the general system (5.1) a quadratic[2] storage function $V(x) = \frac{1}{2} x^T P x$ associated to a symmetric and positive definite matrix $P = P^T > 0$. Also, we adopt the same supply function[3]

$$\mathsf{s}(u,y) = u^T y = y^T u = \frac{1}{2}(u^T y + y^T u). \tag{5.7}$$

Imposing the dissipation inequality in differential form (5.4) leads to

$$\frac{d}{dt}\left\{\frac{1}{2} x^T P x\right\} = \frac{1}{2}(\dot{x}^T P x + x^T P \dot{x}) \leq \frac{1}{2}(u^T y + y^T u) \tag{5.8}$$

and using (5.1) to eliminate $\dot{x}$ and y, we obtain the following condition:

$$\begin{pmatrix} x \\ u \end{pmatrix}^T \begin{pmatrix} A^T P + PA & PB - C^T \\ B^T P - C & -D - D^T \end{pmatrix} \begin{pmatrix} x \\ u \end{pmatrix} \leq 0, \quad P = P^T > 0, \tag{5.9}$$

2 It is well known [89] that, if a storage function V satisfying (5.3) for system (5.1) exists, it can be found as a positive definite quadratic form.

3 In many physical systems power is expressed as the product of relevant variables, such as voltage–current in electrical circuits, pressure–flow in hydraulic systems, and force–velocity in mechanical systems.

which provides the passivity condition to the state-space system (5.1). This condition leads to the well-known *Positive Real Lemma (PRL)*, which is a particular case of the *Kalman–Yakubovich–Popov (KYP) lemma* [51, 66, 92] (see also [2, 56, 74]), which states that the state-space system (5.1) is passive if and only if

$$\exists P = P^T > 0 : \quad \begin{pmatrix} A^T P + PA & PB - C^T \\ B^T P - C & -D - D^T \end{pmatrix} \leq 0. \tag{5.10}$$

This class of conditions is generally known as *Linear Matrix Inequalities (LMIs)* [2, 13, 14, 87]. For a strictly passive (dissipative) system (5.10) holds with a strict inequality.

5.2.1.2 Frequency-domain inequalities

An equivalent condition for passivity characterization is provided by a frequency-domain inequality. It is well known [2, 81, 90] that the transfer function of a general passive system must be *Positive Real (PR)*, i. e., the following three conditions must hold:

1. $H(s)$ must be regular in the open right half complex plane $\Re\{s\} > 0$;
2. $H(s^*) = H^*(s)$, where * denotes the complex conjugate;
3. $\Psi(s) = H(s) + H^T(-s) \geq 0$ for $\Re\{s\} > 0$.

Condition 1 is directly related to the stability of $H(s)$, which is here assumed a priori; condition 2 implies that the impulse response of the system is real-valued; condition 3 completes passivity characterization through a Frequency-Domain Inequality. The connection between the PR conditions and the PRL/KYP Lemma are well-developed and proved in [2].

Since by our assumption all the poles of $H(s)$ are strictly stable, and since the adopted state-space realization is real-valued, both conditions 1 and 2 are automatically satisfied, whereas condition 3 can be restricted to the imaginary axis $s = \jmath\omega$ by the minimum principle of harmonic functions [69], showing that

$$\Psi(\jmath\omega) = H(\jmath\omega) + H^H(\jmath\omega) \geq 0 \quad \forall \omega \in \mathbb{R} \tag{5.11}$$

where ^{H} denotes Hermitian transpose and $\jmath$ is the imaginary unit. Continuing on the same RLC circuit example above, the latter condition states that the input admittance (matrix) of the circuit block must be nonnegative (Hermitian) definite, which in the scalar case $M = 1$ reduces to the requirement that the real part of the input admittance or impedance of any passive one-port element must be nonnegative at any frequency. Condition (5.11) can be further conveniently rewritten as

$$\lambda_i \geq 0, \quad \forall \lambda_i \in \lambda\big(\Psi(\jmath\omega)\big), \quad \forall \omega \in \mathbb{R}, \tag{5.12}$$

where $\lambda(\cdot)$ denotes the set of all eigenvalues of its matrix argument. Nonnegativity can thus be tested for all individual frequency-dependent eigenvalue trajectories $\lambda_i(\jmath\omega)$ of $\Psi(\jmath\omega)$, for $1 \leq i \leq M$. Inequalities (5.11) and (5.12) are strict for $\omega \in \mathbb{R} \cup \{\infty\}$ in the case of strictly passive systems.

5.2.1.3 Hamiltonian matrices

There is a third class of conditions that can be used to characterize a passive system, based on the so-called Hamiltonian matrix associated to (5.1). We introduce this matrix by finding the set of spectral zeros of $\Psi(s)$. Let us assume that $\Psi(s_0)\, v = 0$ for some vector $v \neq 0$, with $s_0 \in \mathbb{C}$. Using (5.2) we have

$$[C(s_0 I - A)^{-1}B + D + B^T(-s_0 I - A^T)^{-1}C^T + D^T]v = 0. \tag{5.13}$$

Let us define

$$\begin{aligned} r &= (s_0 I - A)^{-1}Bv \quad &\rightarrow \quad s_0 r &= Ar + Bv, \\ q &= (-s_0 I - A^T)^{-1}C^T v \quad &\rightarrow \quad s_0 q &= -A^T q - C^T v. \end{aligned} \tag{5.14}$$

Substituting in (5.13) and solving for v under the assumption that $W_0 = D + D^T$ is nonsingular (see Section 5.6 for a generalization) leads to

$$v = -W_0^{-1}(Cr + B^T q), \tag{5.15}$$

which, inserted in (5.14), again leads to

$$\underbrace{\begin{pmatrix} A - BW_0^{-1}C & -BW_0^{-1}B^T \\ C^T W_0^{-1}C & -A^T + C^T W_0^{-1}B^T \end{pmatrix}}_{\mathcal{M}} \begin{pmatrix} r \\ q \end{pmatrix} = s_0 \begin{pmatrix} r \\ q \end{pmatrix}. \tag{5.16}$$

The matrix $\mathcal{M}$ in (5.16) has (real) Hamiltonian structure, since

$$(J\mathcal{M})^T = J\mathcal{M} \quad \text{where } J = \begin{pmatrix} 0 & I \\ -I & 0 \end{pmatrix}. \tag{5.17}$$

It is easily shown that the corresponding eigenspectrum is symmetric with respect to both real and imaginary axis. Condition (5.16) states that the spectral zeros of $\Psi(s)$ are the eigenvalues of the Hamiltonian matrix $\mathcal{M}$. If one of such eigenvalues is purely imaginary $s_0 = \jmath\omega_0$, then we may have a violation of the frequency-domain inequality (5.12). In fact, if (5.16) holds for some purely imaginary $s_0 = \jmath\omega_0$, then $\Psi(\jmath\omega)$ is singular at ω_0, implying that one of its eigenvalues $\lambda_i(\jmath\omega)$ vanishes at ω_0. If this zero is simple, then the eigenvalue trajectory $\lambda_i(\jmath\omega)$ changes sign at ω_0, thus violating the passivity condition (5.12).

The above observations can be summarized in the following statements [12, 33]. Assuming that A is asymptotically stable, and that $W_0 = D + D^T > 0$ is strictly positive definite, then system (5.1) is strictly passive if and only if the Hamiltonian matrix $\mathcal{M}$ in (5.16) has no purely imaginary eigenvalues. In presence of purely imaginary eigenvalues, the system is passive only if the associated Jordan blocks have even size, in which case it can be shown that the corresponding eigenvalue trajectory $\lambda_i(\jmath\omega)$ does not change sign at ω_0. A qualitative illustration of the above statements is provided by Figure 5.2. For a more complete treatment, which is outside the scope of this introductory chapter, see [1, 54]. We remark that the condition $W_0 > 0$ is equivalent to requiring that the system is asymptotically passive, so that the transfer function is nonnegative Hermitian for $\omega \to \infty$.

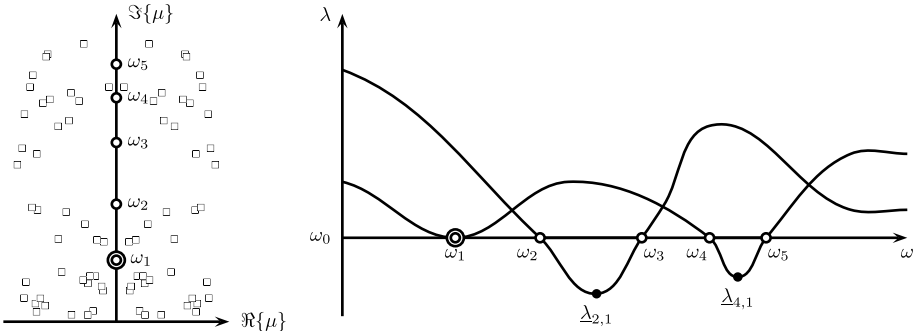

Figure 5.2: Illustration of the relationship between Hamiltonian eigenvalues μ_k (left) and eigenvalues $\lambda_i(\jmath\omega)$ of $\Psi(\jmath\omega)$ (right). In the left panel, purely imaginary Hamiltonian eigenvalues are denoted with circles (number of circles denote multiplicity) to distinguish them from other eigenvalues (squares); only eigenvalues with nonnegative imaginary part are shown. In the right panel, the nonpassive frequency bands $\Omega_2 = (\omega_2, \omega_3)$ and $\Omega_4 = (\omega_4, \omega_5)$ are highlighted with a thick line, with corresponding local minima $\underline{\lambda}_{2,1}$ and $\underline{\lambda}_{4,1}$.

5.3 Checking passivity

There are two main approaches for checking whether a given state-space model (5.1) is passive. These methods exploit the Positive Real Lemma (5.10) and the properties of the Hamiltonian matrix (5.16), respectively.

5.3.1 Checking passivity via linear matrix inequalities

The Positive Real Lemma discussed in Section 5.2.1.1 states that system (5.1) is passive if and only if (5.10) holds. Note that this condition embeds as a corollary also a stability

check, since restricting (5.10) to its upper-left block, which corresponds to setting $u = 0$, i. e., considering the zero-input response, results in the popular Lyapunov condition for (simple) stability, here restricted to the LTI case, which reads

$$\exists P = P^T > 0 : \quad A^T P + PA \leq 0. \tag{5.18}$$

Both (5.18) and (5.10) are recognized as *LMI feasibility* (convex) problems. As such, they can be readily solved by specialized LMI convex optimization software, such as SeDuMi [77] and Yalmip [55]. For a survey of tools see [49], part 6. If the system is passive, such tools will return a Lyapunov matrix P for which the above conditions are satisfied. Conversely, they will return a certificate of non-feasibility, thus proving existence of passivity violations.

The main advantage of the LMI-based passivity check is simplicity: one does not have to write any particular code, since most LMI solvers have simple-to-use interfaces. This advantage is counterbalanced by two important drawbacks. The first disadvantage is computational complexity. The PRL in (5.10) requires proving nonnegativity of a $M + N$ matrix, with P being unknown. The number of decision variables is $N(N+1)/2$, i. e., the number of elements of P. A direct implementation thus requires a computational cost that scales as $\mathcal{O}(N^6)$, although advanced solvers exist that can reduce this cost to $\mathcal{O}(N^4)$ [82]. Exploitation of sparsity, structure and symmetries can be used to reduce this cost even further in many practical cases (for an example see [21]).

The second main disadvantage of LMI-based passivity checks is in the binary nature of their output (passive/non-passive). If the system is not passive, no additional information is available from the solver that can be exploited to fix the passivity violation by a suitable perturbation process. Fortunately, this information is available from the Hamiltonian-based passivity check, discussed next.

5.3.2 Checking passivity using Hamiltonian eigenvalues

As discussed in Section 5.2.1.3, an asymptotically stable system (5.1) with $D + D^T > 0$ is passive if the Hamiltonian matrix $\mathcal{M}$ defined in (5.16) does not have purely imaginary eigenvalues with odd-sized Jordan blocks (in the vast majority of cases these eigenvalues, if any, are simple). This suggests a simple algorithm for checking passivity, summarized as pseudocode in Algorithm 5.1. This scheme is formulated so that it provides as output some additional information, in particular the frequency bands where (5.12) is violated [33]. This information will prove very useful in Section 5.5 for removing such passivity violations via perturbation.

As a first step, we form the Hamiltonian matrix and we compute its eigenvalues $\mu_k \in \text{eig}(\mathcal{M})$. If no such eigenvalues are purely imaginary, and if $D + D^T > 0$, then the model is concluded to be strictly passive and the algorithm stops. No eigenvalue trajectory will cross the imaginary axis, otherwise the corresponding intersection would be pinpointed by some imaginary Hamiltonian eigenvalue.

The more interesting case occurs in the presence of purely imaginary eigenvalues $\mu_k = \jmath\omega_k$. Let us extract the subset of these eigenvalues with nonnegative imaginary part (recall that, if $\jmath\omega_k$ is an eigenvalue, also $-\jmath\omega_k$ is an eigenvalue due to the Hamiltonian structure of $\mathcal{M}$) and sort them in ascending order,

$$0 = \omega_0 < \omega_1 < \omega_2 < \cdots < \omega_K < \omega_{K+1} = +\infty \tag{5.19}$$

where ω_0 is added even if 0 is not an eigenvalue of $\mathcal{M}$, and where we set $\omega_{K+1} = +\infty$. The frequencies ω_k induce a partition of the frequency axis into disjoint adjacent subbands $\Omega_k = (\omega_k, \omega_{k+1})$ for $k = 0, \ldots, K$. From the above discussion, $\Psi(\jmath\omega)$ is nonsingular $\forall\omega \in \Omega_k$, $\forall k$.

Each subband Ω_k is then flagged as passive or non-passive by assigning k to corresponding index sets $\mathcal{K}_p$ and $\mathcal{K}_{np}$, respectively, depending on whether (5.12) is verified or not for $\omega \in \Omega_k$. This condition is very easy to check, due to the continuity of all eigenvalue trajectories $\lambda_i(\jmath\omega)$, which is a consequence of the assumed asymptotic stability, so that both $H(s)$ and $\Psi(s)$ are regular on the imaginary axis. It is thus sufficient to check whether

$$\Psi(\jmath\check{\omega}_k) > 0, \quad \text{where } \check{\omega}_k = \frac{\omega_k + \omega_{k+1}}{2}, \tag{5.20}$$

is the midpoint of band Ω_k. If (5.20) is verified, then the model is uniformly passive in Ω_k and $k \in \mathcal{K}_p$. Otherwise, $k \in \mathcal{K}_{np}$ and the number of negative eigenvalues $\lambda_i(\jmath\omega)$ (which is constant in Ω_k), is determined based on their evaluation at the midpoint $\check{\omega}_k$.

As a final optional step, the subbands Ω_k with $k \in \mathcal{K}_{np}$ can be subjected to a local (adaptive) sampling in order to find all local minima of the eigenvalue trajectories $\lambda_i(\jmath\omega)$. These minima, denoted with their frequency location as $(\underline{\omega}_{kv}, \underline{\lambda}_{kv})$, correspond to the worst-case local passivity violations. See Figure 5.2 for a graphical illustration. See also [20, 34].

The computational cost of the passivity check in Algorithm 5.1 is dominated by the Hamiltonian eigenvalue evaluation. A general-purpose eigenvalue solver scales as $\mathcal{O}(\kappa N^3)$ where κ is a constant, since the size of the Hamiltonian matrix (5.16) is $2N$. Specialized eigensolvers exist that reduce this cost by exploiting the particular matrix structure [7, 10]; see also [1, 9, 79], but still retaining the scaling $\mathcal{O}(\kappa N^3)$ albeit with a smaller constant κ. If the transfer function $H(s)$ of the model is symmetric (which is usually verified in electrical and electronic applications), additional computational savings can be achieved by defining equivalent and smaller-size eigenproblems, often referred to as *half-size passivity tests*; see [23, 36, 47, 48, 75].

When the number of states N is medium-large and the state-space realization is sparse (for instance with A diagonal or quasi-diagonal), then it is more convenient to use eigensolvers based on repeated shift-invert iterations; see e. g. [3, 41, 85]. It has been demonstrated that these methods are able to reduce the scaling law of purely imaginary eigenvalue determination to $\mathcal{O}(\kappa N)$, although with a possibly large κ. See also [8, 60, 85] for details on more general structured eigenproblems.

Algorithm 5.1: Hamiltonian-based passivity check.

Require: real state-space matrices A, B, C, D
Require: A asymptotically stable, $D + D^T$ nonsingular
1: form the Hamiltonian matrix $\mathcal{M}$ of (5.16) and compute its eigenvalues μ_k
2: **if** no eigenvalue is purely imaginary and $D + D^T > 0$ **then**
3: system is strictly passive: exit
4: **end if**
5: extract all imaginary eigenvalues $\mu_k = \jmath\omega_k$ and sort them as in (5.19)
6: set $\mathcal{K}_p = \mathcal{K}_{np} = \emptyset$
7: **for** $k = 0, \ldots, K$ **do**
8: form subband $\Omega_k = (\omega_k, \omega_{k+1})$ and its midpoint $\breve{\omega}_k$
9: **if** $\Psi(\jmath\breve{\omega}_k) > 0$ **then**
10: system is locally passive $\forall\omega \in \Omega_k$, add k to $\mathcal{K}_p$
11: **else**
12: system is not passive in Ω_k, add k to $\mathcal{K}_{np}$
13: find all local minima $(\underline{\omega}_{kv}, \underline{\lambda}_{kv})$ of the eigenvalues of $\Psi(\jmath\omega)$ in Ω_k
14: **end if**
15: **end for**

5.4 System perturbation

Assuming that the system (5.1) is detected as non-passive from a passivity check, the main question arises whether we can enforce its passivity through a small perturbation of its coefficients. What is actually important is not the amount of coefficient perturbation, but rather the perturbation in the model response, which should be kept under control in order to maintain model accuracy. Of course, this approach makes sense only if the passivity violations of the initial model are relatively small to enable correction via perturbation. This situation is in fact commonly encountered in applications. Very large passivity violations in models that should represent dissipative systems are a clear indication of poor model quality. Such models should be discarded and regenerated.

Several perturbation approaches are possible for (5.1). In the following, we focus on one particular strategy, which amounts to perturbing only the state-output matrix as $\hat{C} = C + \delta C$ while leaving the other state-space matrices unchanged. This strategy induces the following perturbation in the transfer function:

$$\hat{H}(s) = H(s) + \delta H(s) \quad \text{with } \delta H(s) = \delta C(sI - A)^{-1}B. \tag{5.21}$$

The corresponding impulse response perturbation is thus

$$\hat{h}(t) = h(t) + \delta h(t) \quad \text{with } \delta h(t) = \delta C e^{At} B\mathrm{u}(t) \tag{5.22}$$

where u is the Heaviside step function. This approach leaves the state matrix A unchanged, thus preserving the system poles. Allowing for poles perturbation induced by a modification of A would require in fact additional constraints for ensuring that stability is not compromised. Except for very few cases [22, 53], most existing passivity enforcement schemes do not modify matrix A in order to preserve the system poles. This is a common scenario in those applications where passivity enforcement is applied as a post-processing of a model identified from measurements with Vector Fitting (see [5, Chapter 8]). If the system is asymptotically passive with $D + D^T > 0$, there is also no need to modify the direct coupling matrix D. Modification of the input-state map B can be considered as an alternative to (5.21).

Based on (5.21), we need to determine a cost function that measures the perturbation amount in terms of the decision variables, i. e., the elements of δC. A number of popular cost functions are reviewed below.

5.4.1 Gramian-based cost functions

A natural choice for measuring the system perturbation is the L_2 norm. We have

$$\mathcal{E}_2^2 = \|\delta h\|_{L_2}^2 = \int_0^{+\infty} \operatorname{tr}\big(\delta h(t)\delta h(t)^T\big)\, dt = \operatorname{tr}\big(\delta C \mathcal{G}_c \delta C^T\big) \tag{5.23}$$

where tr is the trace of its matrix argument, and

$$\mathcal{G}_c = \int_0^{+\infty} e^{At} B B^T e^{A^T t}\, dt = \frac{1}{2\pi} \int_{-\infty}^{+\infty} (\jmath\omega I - A)^{-1} B B^T (\jmath\omega I - A)^{-H}\, d\omega \tag{5.24}$$

is the *Controllability Gramian* of the system, which is easily found by solving the Lyapunov equation

$$A\mathcal{G}_c + \mathcal{G}_c A^T = -BB^T. \tag{5.25}$$

Although simple to use, the cost function (5.23) is seldom used in applications. This is due to the fact that most often a reduced order model is obtained from some approximation process that ensures accuracy only in a well-defined frequency band, which usually does not extend up to ∞. Assuming that the model accuracy is of interest only for $\omega \in [0, \omega_{\max}]$, then it is unnecessary and even detrimental to include any contribution to the Gramian coming from frequencies $|\omega| > \omega_{\max}$. A simple approach to obtain a bandlimited norm is to limit the integration bounds in (5.24) to $\mp\omega_{\max}$. One loses the possibility to compute $\mathcal{G}_c$ through (5.25), so that the corresponding bandlimited Gramian should be obtained by a direct numerical integration of (5.24) through some quadrature rule.

An alternative option is to introduce a nonnegative weighting function $\rho(\omega)$ in the frequency-domain integral (5.24), which allows one to fine-tune the contributions to the Gramian coming from different frequencies. The latter strategy lends itself to a simple algebraic procedure for the weighted Gramian computation, in the case the weight is restricted to be in form of a state-space system applied to the input or to the output of our original transfer function $H(s)$. Some details follow.

Let us consider a weighting function in state-space form with transfer matrix $\Gamma(s) = C_\Gamma(sI - A_\Gamma)^{-1}B_\Gamma + D_\Gamma$ of compatible size, which is applied to defining a *weighted error function*

$$\delta H_\Gamma(s) = \delta H(s)\,\Gamma(s). \tag{5.26}$$

Instead of (5.23), we measure system perturbation through the Γ-weighted norm defined as

$$\mathcal{E}_\Gamma^2 = \|\delta H\|_\Gamma^2 = \|\delta H_\Gamma\|_{L_2}^2. \tag{5.27}$$

It can be easily shown [99] that this norm can be computed as

$$\|\delta H\|_\Gamma^2 = \mathrm{tr}(\delta C\, P_\Gamma\, \delta C^T), \tag{5.28}$$

where P_Γ is the upper-left block of the solution of the following augmented Lyapunov equation:

$$\tilde{A}\,\tilde{P} + \tilde{P}\,\tilde{A}^T = -\tilde{B}\tilde{B}^T \tag{5.29}$$

with

$$\tilde{A} = \begin{pmatrix} A & BC_\Gamma \\ 0 & A_\Gamma \end{pmatrix}, \quad \tilde{B} = \begin{pmatrix} BD_\Gamma \\ B_\Gamma \end{pmatrix}, \quad \tilde{P} = \begin{pmatrix} P_\Gamma & P_{12} \\ P_{12}^T & P_{22} \end{pmatrix}. \tag{5.30}$$

We see that this characterization is fully compatible with the standard L_2 norm, as far as the standard Gramian $\mathcal{G}_c$ is replaced by its weighted counterpart P_Γ. This formulation can be adapted to applications that require control over relative error, by choosing $\Gamma(s) = H^{-1}(s)$ or even elementwise relative error [42]. If we are interested in retaining accuracy only in some prescribed frequency band $(\omega_{\min}, \omega_{\max})$, then $\Gamma(s)$ can be defined as a band pass filter matched to this band.

The two Gramian-based error characterizations (5.23) and (5.28) are further simplified as follows. Let us consider (5.23), and let us assume that the initial model is controllable, so that the controllability Gramian $\mathcal{G}_c$ is full-rank and strictly positive definite.[4] Computing the Cholesky factorization $\mathcal{G}_c = Q_c^T Q_c$ and inserting it into (5.23) leads to

$$\mathcal{E}_2^2 = \mathrm{tr}(\delta C\, Q_c^T Q_c\, \delta C^T) = \mathrm{tr}(\Xi\,\Xi^T) = \|\Xi\|_F^2 = \|\xi\|_2^2 \tag{5.31}$$

4 In case $\mathcal{G}_c$ is singular, a preprocessing step based, e. g., on Balanced Truncation [5, Chapter 2] can be applied to remove any uncontrollable states.

where $\|\cdot\|_F$ denotes the Frobenius norm of its matrix argument, $\Xi = \delta C\, Q_c^T$ and $\xi = \mathrm{vec}(\Xi)$ stacks the columns of Ξ into a single column vector.[5] We see that the model perturbation is now cast as the Euclidean norm of the (vectorized) decision variables ξ in a new coordinate system induced by the Cholesky factor of the Gramian. Minimization of (5.31) is thus trivial.

5.4.2 Data-based cost functions

A further alternative for defining a cost function that measures the model perturbation error is based on a purely discrete formulation. Let us suppose that the model (5.1) was obtained in first place through a data-driven MOR scheme, starting form a set of frequency-domain measurements of the underlying system response $(\omega_\ell, \breve{H}_\ell)$ for $\ell = 1, \ldots, L$. A natural choice would be to minimize the error of the perturbed model with respect to these initial data [21, 43, 44, 46]

$$\mathcal{E}^2 = \sum_{\ell=1}^{L} \rho_\ell^2 \mathcal{E}_\ell^2 \quad \text{with } \mathcal{E}_\ell^2 = \|H(\jmath\omega_\ell) + \delta H(\jmath\omega_\ell) - \breve{H}_\ell\|_F^2, \tag{5.32}$$

where we used the Frobenius norm to define the local error $\mathcal{E}_\ell$ for each frequency point (of course other norm choices are possible), and where ρ_ℓ is a weighting factor to be defined based on the desired approximation criteria. A straightforward derivation shows that, vectorizing the decision variables as $\delta c = \mathrm{vec}(\delta C)$, we can write

$$\mathcal{E}^2 = \|K\delta c - d\|_2^2 \tag{5.33}$$

with

$$K^T = \begin{pmatrix} \rho_1 K_1^T & \cdots & \rho_L K_L^T \end{pmatrix}, \quad d^T = \begin{pmatrix} \rho_1 d_1^T & \cdots & \rho_L d_L^T \end{pmatrix}, \tag{5.34}$$

where the various components are defined using the Kronecker product $\otimes$ as

$$K_\ell = \left[(\jmath\omega_\ell I - A)^{-1} B\right]^T \otimes I, \quad d_\ell = \mathrm{vec}\big(H(\jmath\omega_\ell) - \breve{H}_\ell\big). \tag{5.35}$$

A particular case of (5.32) is obtained by defining

$$\mathcal{E}_\ell^2 = \|\delta H(\jmath\omega_\ell)\|_F^2. \tag{5.36}$$

This choice corresponds to setting the "target" data samples as the responses of the initial model, so that $\breve{H}_\ell = H(\jmath\omega_\ell)$ and consequently $d_\ell = 0$. Correspondingly, (5.33) reduces to the simple quadratic form

$$\mathcal{E}^2 = \|K\delta c\|_2^2. \tag{5.37}$$

5 We will denote the inverse operation $\Xi = \mathrm{mat}(\xi)$, where the size of Ξ is inferred from the context.

5.5 Passivity enforcement

In Section 5.4, we showed how the perturbation of a model based on a modification of the state-output map can be algebraically characterized as a quadratic form of the decision variables, i. e., the elements of δC, possibly cast in a different coordinate system. The resulting cost function provides an effective control over model perturbation if used within an optimization problem, combined with suitable constraints for passivity enforcement. In this section, we discuss the three most prominent approaches for casting the passivity conditions introduced in Section 5.2.1 as constraints, giving rise to three classes of algorithms for passivity enforcement. An overview of alternative approaches and a more complete treatment is available in [39].

5.5.1 Passivity enforcement via LMI constraints

Let us consider an initial non-passive system (5.1), for which the PRL condition (5.10) is not satisfied. We try to enforce this condition on a perturbed system, where the state-output matrix C is updated as

$$\hat{C} = C + \delta C = C + \Xi Q_c^{-T}, \tag{5.38}$$

where we used the change of variables in (5.31) based on the Cholesky factor Q_c of the controllability Gramian. Enforcing the PRL for the perturbed system while minimizing the perturbation, based, e. g., on the cost function (5.31), amounts to solving the following constrained optimization problem

$$\min_{P,\Xi} \|\Xi\|_F^2 \quad \text{s. t.} \quad P = P^T > 0 \quad \text{and} \quad \mathcal{F}(P,\Xi) \leq 0 \tag{5.39}$$

where

$$\mathcal{F}(P,\Xi) = \begin{pmatrix} A^T P + PA & PB - C^T - Q_c^{-1}\Xi^T \\ B^T P - C - \Xi Q_c^{-T} & -D - D^T \end{pmatrix}. \tag{5.40}$$

The cost function in (5.39) is a quadratic form in the decision variables, and both constraints are of LMI type [21]. Problem (5.39) is known to be convex, therefore there is a theoretical guarantee that a unique optimal solution exists, which can be found in polynomial time. In fact, specialized solvers for this class of problems exist, see e. g. [55, 77], therefore we do not detail any particular algorithm any further (see also section 5.3.1). The reader is referred to standard textbooks on convex optimization for more details [14].

As already discussed in Section 5.3.1, the computational cost that is required to solve (5.39) scales quite badly with the number of decision variables, equivalently with the system size. The main motivation for this high computational requirements is the

presence of the Lyapunov matrix P in the set of decision variables, which is only instrumental to the PRL formulation, but which is not really needed as a result of the optimization process. Therefore, we can think of eliminating P with a suitable preprocessing step, in order to obtain a smaller LMI problem that can be solved more efficiently. The so-called *trace parameterization* provides a solution to this problem; see [25, 21, 18] for details. We now seek alternatives that provide even better scalability. The reader is encouraged to also see [43].

5.5.2 Passivity enforcement via Hamiltonian perturbation

Let us consider the Hamiltonian-based passivity constraints discussed in Section 5.2.1.3. Under the assumptions that A is asymptotically stable and system (5.1) is asymptotically passive with $D + D^T > 0$, then (strict) passivity holds if the Hamiltonian matrix $\mathcal{M}$ in (5.16) has no purely imaginary eigenvalues. If this is not true, as Figure 5.2 shows, the Hermitian part of the frequency response has some negative eigenvalues in some frequency bands, and the system is not passive due to those localized violations.

The main idea of passivity enforcement via Hamiltonian perturbation is to induce a spectral perturbation on the imaginary Hamiltonian eigenvalues, so that they are displaced in the correct direction as to eliminate the local passivity violations [33]. A graphical illustration of this strategy is provided in Figure 5.3, where we show that when two imaginary eigenvalues are displaced along the imaginary axis in a direction that points inward each passivity violation band, the extent of the violation is effectively reduced (top panels). If the perturbation amount is sufficiently large to induce a collision of the two imaginary eigenvalues (bottom panels), then a bifurcation occurs and the two eigenvalues move off the imaginary axis. The passivity violation is thus removed.

The above spectral perturbation is an inverse problem, which requires a precise characterization of the relation between matrix element perturbations and the corresponding induced change in the eigenvalues that we need to displace. The algorithm that we describe below is based on a first-order approximation of this relation.

Let us consider once again a non-passive system which is perturbed by changing the state-output matrix as $\hat{C} = C + \delta C$. A straightforward first-order approximation analysis leads to the following expression for the perturbed Hamiltonian matrix:

$$\hat{\mathcal{M}} = \mathcal{M} + \delta\mathcal{M} \quad \text{with } \delta\mathcal{M} \approx \begin{pmatrix} -BW_0^{-1}\delta C & 0 \\ C^T W_0^{-1}\delta C + \delta C^T W_0^{-1} C & \delta C^T W_0^{-1} B^T \end{pmatrix} \tag{5.41}$$

where $W_0 = D + D^T$. Let us now consider a generic eigenvalue μ_k of $\mathcal{M}$ with unit multiplicity, and let us denote the corresponding right and left eigenvectors as v_k and w_k, normalized such that $\|v_k\| = \|w_k\| = 1$. We have the following first-order eigenvalue

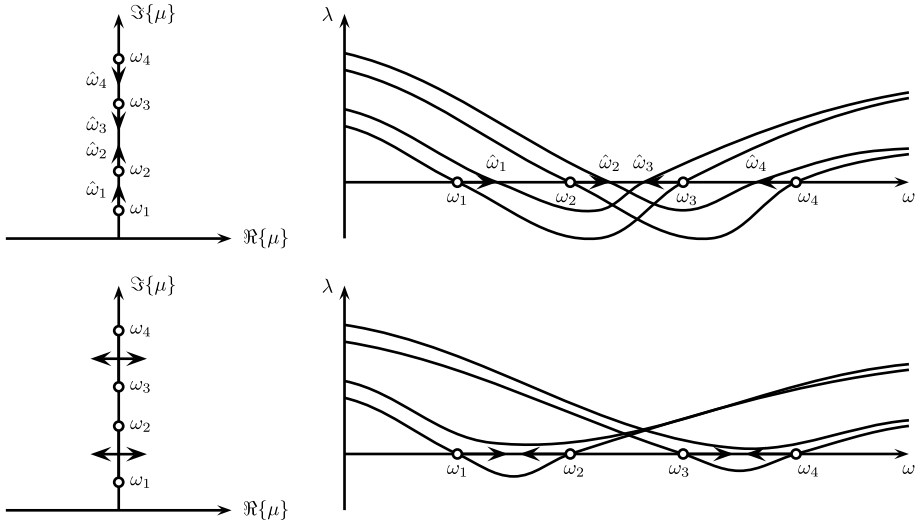

Figure 5.3: Illustration of passivity enforcement via Hamiltonian eigenvalue perturbation. Top and bottom panels refer to two different scenarios that may occur. In the top left panel the purely imaginary Hamiltonian eigenvalues are depicted with empty dots, and their perturbation direction and extent is represented with thick arrows. The corresponding eigenvalue trajectories $\lambda_i(\jmath\omega)$ before (solid lines) and after (dashed lines) perturbation are depicted in the top right panel. Bottom panels show that when two imaginary Hamiltonian eigenvalues collide (left panel), the corresponding intersections of the eigenvalue trajectories $\lambda_i(\jmath\omega)$ with the frequency axis are removed (right panel).

perturbation result [86]:

$$\hat{\mu}_k \approx \mu_k + \delta\mu_k \quad \text{with} \quad \delta\mu_k = \frac{w_k^H \delta\mathcal{M}\, v_k}{w_k^H v_k}. \tag{5.42}$$

We now particularize (5.42) to the case of a purely imaginary eigenvalue $\mu_k = \jmath\omega_k$. It is well known that, for such eigenvalues, the left and right eigenvectors are related by $w_k = -Jv_k$, where J is defined in (5.17), so that we can write

$$\delta\mu_k = \frac{v_k^H J\, \delta\mathcal{M}\, v_k}{v_k^H J\, v_k}. \tag{5.43}$$

Splitting now the right eigenvector as $v_k^T = (v_{k1}^T, v_{k2}^T)$ according to the block structure of $\mathcal{M}$, we see that the denominator of (5.43) is purely imaginary

$$v_k^H J\, v_k = 2\jmath\,\mathbb{I}\{v_{k1}^H v_{k2}\} \tag{5.44}$$

whereas the numerator is real-valued since $J\mathcal{M}$ is real and symmetric. A tedious but straightforward calculation leads to

$$v_k^H J\, \delta\mathcal{M}\, v_k = 2\mathbb{R}\{v_{k1}^T \otimes y_k^H\}\, \delta c \tag{5.45}$$

where $\delta c = \mathrm{vec}(\delta C)$ and the auxiliary vector y_k is defined as

$$y_k = W_0^{-1}(Cv_{k1} + B^T v_{k2}). \tag{5.46}$$

Using the above expressions, we can finally rewrite (5.43) as

$$\Re\{v_{k1}^T \otimes y_k^H\}\,\delta c \approx (\omega_k - \hat{\omega}_k)\Im\{v_{k1}^H v_{k2}\}, \tag{5.47}$$

where we used the fact that under the adopted first-order approximation also the perturbed eigenvalue is purely imaginary $\hat{\mu}_k = \jmath\hat{\omega}_k$. Furthermore, applying the change of variables (5.31) to (5.47) gives

$$z_k^T \xi \approx \eta_k \tag{5.48}$$

where

$$z_k = \Re\{(Q_c^{-T} v_{k1}) \otimes y_k^*\}, \quad \eta_k = (\omega_k - \hat{\omega}_k)\Im\{v_{k1}^H v_{k2}\}. \tag{5.49}$$

This expression is a linearized constraint that relates the amount of (imaginary) eigenvalue perturbation to the corresponding perturbation on the decision variables ξ.

When using (5.48) as a constraint to determine ξ, the desired location for $\hat{\omega}$ needs to be provided as input. With reference to Figure 5.3, we see that the direction where ω_k should be perturbed is directly related to the slope $\lambda'_{i,k}$ of the eigenvalue trajectory $\lambda_i(\jmath\omega)$ that vanishes at ω_k. A heuristic yet effective choice for $\hat{\omega}_k$ is

$$\begin{cases} \hat{\omega}_k = \omega_k + \alpha(\omega_{k+1} - \omega_k) & \text{for } \lambda'_{i,k} < 0, \\ \hat{\omega}_k = \omega_k - \alpha(\omega_k - \omega_{k-1}) & \text{for } \lambda'_{i,k} > 0, \end{cases} \tag{5.50}$$

where the control parameter $0 < \alpha < 1$ determines the maximum extent of the perturbation amount relative to the size of the violation subband. Additional details on how to determine the slopes $\lambda'_{i,k}$ as well as appropriate values of α can be found in [33].

Supposing now that multiple eigenvalues $\mu_k = \jmath\omega_k$ for $k = 1, \ldots, K$ are to be perturbed concurrently, we need to collect all independent constraints (5.48) so that they are enforced simultaneously. The resulting optimization problem to be solved reads

$$\min_{\xi} \|\xi\|_2^2 \quad \text{s. t.} \quad z_k^T \xi = \eta_k, \quad k = 1, \ldots, K \tag{5.51}$$

This is a simple linearly constrained minimum norm problem, whose optimal solution is $\xi_{\mathrm{opt}} = Z^\dagger \eta$, where † denotes the pseudoinverse [14], with Z and η collecting z_k^T and η_k as rows. Compared to the evaluation of the Hamiltonian eigenvalues required to set up the constraints (5.48), the solution of (5.51) has a negligible computational cost.

Although the solution of (5.51) is straightforward, its passivity constraint is based on a linearization process and is therefore only accurate up to first order. Therefore,

the perturbation fraction α should be selected to be small enough for the first-order approximation to be accurate, and multiple iterations may be required to displace all imaginary eigenvalues. Figure 5.3 illustrates two scenarios that may typically occur during iterations, whereas Algorithm 5.2 provides the pseudocode of a possible implementation. The computational cost of this implementation is dominated by the Hamiltonian eigensolution; see the discussion in Section 5.3.2. We remark that, despite the fact the optimization problem (5.51) at each iteration has a closed-form solution, the overall iterative scheme in its basic formulation is not guaranteed to converge, since a local perturbation of few eigenvalues does not guarantee that new imaginary eigenvalues will not occur at other locations. The approach that is presented in the next section provides a more robust scheme.

Algorithm 5.2: Passivity enforcement via Hamiltonian perturbation.

Require: real state-space matrices A, B, C, D
Require: A asymptotically stable, $D + D^T > 0$
Require: control parameter $0 < \alpha < 1$ and max iterations $i_{\max}$
run Alg. 5.1 to check passivity, store $\{\omega_k\}$ and non-passive bands Ω_k
compute Gramian $\mathcal{G}_c$ or weighted Gramian P_Γ and its Cholesky factor Q_c
set iteration count $i = 0$
while (system not passive and $i < i_{\max}$) **do**
    $i \leftarrow i + 1$
    compute right eigenvectors v_k and form vectors z_k in (5.49), for all k
    define $\hat{\omega}_k$ as in (5.50) and form η_k in (5.49) for all k
    solve optimization problem (5.51) for ξ
    update state-output map $C \leftarrow C + \Xi Q_c^{-T}$ where $\Xi = \mathrm{mat}(\xi)$
    run Alg. 5.1 to check passivity, store $\{\omega_k\}$ and non-passive bands Ω_k
end while

Before closing this section we remark that the above discussion was based on the assumption of simple Hamiltonian eigenvalues. A full characterization of the general case with arbitrary higher multiplicity requires knowledge of the complete structure of the possibly multiple Jordan blocks of the Hamiltonian matrix. This discussion is outside the scope of this chapter, the reader is referred to [1, 61] for a complete treatment. We only remark that the presence of defective eigenspaces is structurally unstable to small perturbations, so that the defectivity usually disappears if a small perturbation is applied.

Passivity enforcement via Hamiltonian perturbation was first introduced in [33], followed by various applications [17, 31, 71] and extensions to large-scale systems [41]

with possibly frequency weighted accuracy norms [42]. It is worth mentioning the straightforward extension [11, 57] to so-called *negative imaginary* systems.[6]

5.5.3 Passivity enforcement via local perturbation

Let us consider once again a system that is detected as non-passive from Algorithm 5.1. One of the results that this algorithm provides in addition to the index set $k \in \mathcal{K}_{np}$ that identifies the non-passive bands $\Omega_k = (\omega_k, \omega_{k+1})$ is a set of local minima $(\underline{\omega}_{kv}, \underline{\lambda}_{kv})$ of the eigenvalues of $\Psi(\jmath\omega)$ in each of these subbands. Figure 5.4 depicts these local minima with filled dots.

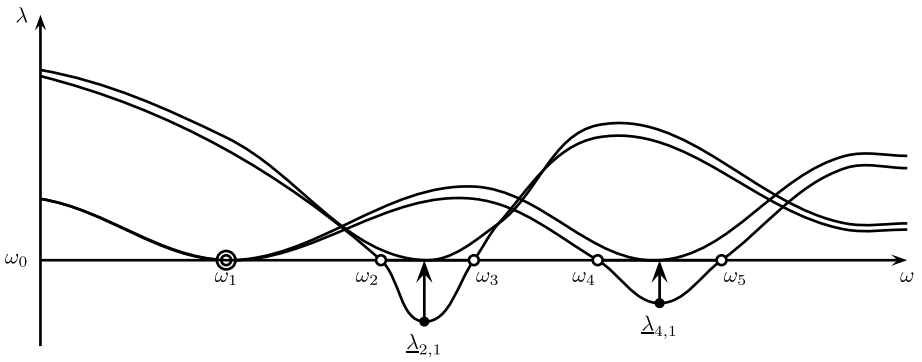

Figure 5.4: Illustration of passivity enforcement via local perturbation. Linearized constraints are used to perturb (thick arrows) the local minima $\underline{\lambda}_{i,k}$ (filled dots) of the eigenvalue trajectories $\lambda_i(\jmath\omega)$ (solid lines) so that they become nonnegative. The resulting perturbed eigenvalue trajectories (dashed lines) are uniformly positive after few iterations.

Assume now to perturb the system through the usual state-output matrix as $\hat{C} = C + \delta C$. This perturbation leads to an induced perturbation on the eigenvalue trajectories $\lambda(\jmath\omega)$, represented in Figure 5.4 by solid lines. We seek a constraint that displaces the local minima to a new nonnegative value [72, 73]. Denoting with v_{kv} the eigenvector of $\Psi(\jmath\underline{\omega}_{kv})$ normalized as $\|v_{kv}\| = 1$ corresponding to the eigenvalue $\underline{\lambda}_{kv}$, we can express the induced eigenvalue perturbation through the following first-order approximation, which results in an inequality constraint after imposing nonnegativity:

$$\hat{\underline{\lambda}}_{kv} = \underline{\lambda}_{kv} + v_{kv}^H \, \delta\Psi(\jmath\underline{\omega}_{kv}) \, v_{kv} \geq 0. \tag{5.52}$$

6 A system with square, strictly proper and stable transfer matrix $H(s)$ is negative imaginary if and only if $sH(s)$ is Positive Real.

Figure 5.4 provides a graphical illustration of the perturbation, together with the expected perturbed eigenvalue trajectories (dashed lines). Note that these trajectories remain continuous after perturbation, thanks to the assumed asymptotic stability of the model (no poles on the imaginary axis).

The constraint (5.52) can now be readily expressed in terms of our decision variables δC, noting that

$$\delta\Psi(\jmath\omega) = \delta C\, T(\jmath\omega) + T^H(\jmath\omega)\, \delta C^T \tag{5.53}$$

where $T(\jmath\omega) = (\jmath\omega I - A)^{-1}B$. Using the vectorized form $\delta c = \mathrm{vec}(\delta C)$ together with the change of variable (5.31) leads to

$$z_{kv}^T\, \xi \geq -\underline{\lambda}_{kv}, \quad \text{with } z_{kv} = 2\Re\{(Q_c^{-T} T(\jmath\underline{\omega}_{kv})\, v_{kv}) \otimes v_{kv}^*\}. \tag{5.54}$$

As a result, we cast our minimum model perturbation subject to local passivity constraints as

$$\min_{\xi} \|\xi\|_2^2 \quad \text{s.t.} \quad z_{kv}^T\, \xi \geq -\underline{\lambda}_{kv}, \quad \forall k \in \mathcal{K}_{np},\ \forall v. \tag{5.55}$$

This problem is convex and is readily solved through off-the-shelf software. Based on the analysis in [43] the computational cost for solving (5.55) can be reduced to $\mathcal{O}(\kappa NM^2)$.

As for the Hamiltonian perturbation passivity enforcement, the above local perturbation is not guaranteed to achieve a passive model after the solution of (5.55). In fact

- the inequality constraint in (5.54) is only first-order accurate and does not guarantee that the perturbed eigenvalue will be nonnegative after applying the computed model correction;
- it is not guaranteed that a local perturbation of all local eigenvalue minima $(\underline{\omega}_{kv}, \underline{\lambda}_{kv})$ will not induce new passivity violations at new locations, in terms of new negative eigenvalue minima.

The first problem can be easily addressed by embedding (5.55) within an iterative scheme that, after solving (5.55), applies model correction and repeats the perturbation until all local eigenvalue minima are nonnegative. The second problem is also easily addressed by the so-called *robust iterations*, described next.

Assume that after model perturbation a new local eigenvalue minimum $\underline{\lambda}_{\text{new}} < 0$ is detected at some frequency $\underline{\omega}_{\text{new}}$ where the model was locally passive before perturbation. If we could enforce the eigenvalues of $\Psi(\jmath\underline{\omega}_{\text{new}})$ to remain nonnegative through an additional constraint together with those in (5.55), then the new violation would not have arisen. This is exactly the main idea of robust iterations, where problem (5.55) is solved only as a preliminary step. All new violations are collected and nonnegativity constraints are formulated as in (5.54) at the corresponding frequencies and added to

the set of already available constraints. This prediction step is repeated until no new violations are introduced. Then iterations continue after the model is updated.

The passivity enforcement scheme based on local perturbations (without robust iterations) is outlined as pseudocode in Algorithm 5.3. More details on the robust iteration scheme are available in [44, 45].

Algorithm 5.3: Passivity enforcement via local perturbations.

Require: real state-space matrices A, B, C, D
Require: A asymptotically stable, $D + D^T > 0$
Require: max iterations $i_{\max}$
1: run Alg. 5.1 to check passivity, store local eigenvalue minima $(\underline{\omega}_{kv}, \underline{\lambda}_{kv})$
2: compute Gramian $\mathcal{G}_c$ or weighted Gramian P_W and its Cholesky factor Q_c
3: set iteration count $i = 0$
4: **while** (system not passive and $i < i_{\max}$) **do**
5: $\quad i \leftarrow i + 1$
6: $\quad$ compute eigenvectors v_{kv} and form vectors z_{kv} in (5.54), for all k, v
7: $\quad$ solve optimization problem (5.55) for ξ
8: $\quad$ update state-output map $C \leftarrow C + \Xi Q_c^{-T}$ where $\Xi = \mathrm{mat}(\xi)$
9: $\quad$ run Alg. 5.1 to check passivity, store local eigenvalue minima $(\underline{\omega}_{kv}, \underline{\lambda}_{kv})$
10: **end while**

5.6 Extensions

The various passivity check and enforcement algorithms discussed in previous sections were restricted to the narrow class of regular state-space systems (5.1), with A asymptotically stable, with $D + D^T > 0$, and with a supply rate defined by (5.7). In this section, we release these assumptions by providing suitable generalizations.

5.6.1 Releasing asymptotic passivity requirements

When $W_0 = D + D^T$ is singular but positive semidefinite, then the system might still be passive (although not strictly passive), with at least one of the eigenvalues $\lambda_i(\jmath\omega)$ of $\Psi(\jmath\omega)$ vanishing for $\omega \to \infty$. In this scenario, the passivity check based on the Hamiltonian matrix $\mathcal{M}$ in (5.16) cannot be performed, since $\mathcal{M}$ is ill-defined and cannot be constructed.

The Hamiltonian matrix can, however, be generalized [93] by avoiding the inversion of W_0 in (5.15). Retaining the vector v and adding it as an additional block-component to the eigenvector in (5.16) leads to the following generalized eigenvalue

problem:

$$\underbrace{\begin{pmatrix} A & 0 & B \\ 0 & -A^T & -C^T \\ C & B^T & W_0 \end{pmatrix}}_{\mathcal{M}} \begin{pmatrix} r \\ q \\ v \end{pmatrix} = s_0 \underbrace{\begin{pmatrix} I & 0 & 0 \\ 0 & I & 0 \\ 0 & 0 & 0 \end{pmatrix}}_{\mathcal{N}} \begin{pmatrix} r \\ q \\ v \end{pmatrix}. \tag{5.56}$$

The pencil $(\mathcal{M}, \mathcal{N})$ has at least one infinite eigenvalue due to the singularity of W_0. However, by the same argument used in Section 5.2.1.3, the finite purely imaginary eigenvalues $\mu_k = \jmath\omega_k$ of the pencil still correspond to the frequencies ω_k where one eigenvalue of Ψ vanishes as $\lambda_i(\jmath\omega_k) = 0$. Therefore, the passivity check detailed in Section 5.3.2 and Algorithm 5.1 can still be applied as far as the Hamiltonian matrix eigenvalue problem (5.16) is replaced by (5.56). Alternative approaches for handling this case, based on frequency transformations, can be found in [23, 72, 76].

5.6.2 Enforcing asymptotic passivity

When $W_0 = D + D^T$ is not sign definite, with at least one negative eigenvalue, most of the foregoing results do not apply if not properly generalized. For instance, the PRL condition (5.10) cannot be satisfied, since the model is not passive at infinite frequency. Therefore, the proposed system perturbation (5.21) for passivity enforcement will not be effective since also matrix D should be modified.

There are two main alternative approaches to recovering strict asymptotic passivity and enable all passivity enforcement schemes discussed in Section 5.5. One approach involves a preprocessing step that first modifies D so that its symmetric part is strictly positive definite. Let us compute the following eigendecomposition:

$$\frac{D + D^T}{2} = V \Lambda V^T \tag{5.57}$$

where $\Lambda = \mathrm{diag}(\lambda_1, \ldots, \lambda_P)$ collects the eigenvalues and V the corresponding eigenvectors. We can simply redefine the eigenvalues in (5.57) as $\hat{\lambda}_p = \max(\lambda_p, \varepsilon)$ where $\varepsilon > 0$ is a prescribed positive minimum value assigned to the eigenvalues. The resulting model

$$H_{ap}(s) = C(sI - A)^{-1}B + \hat{D}, \quad \hat{D} = V\mathrm{diag}(\hat{\lambda}_1, \ldots, \hat{\lambda}_P)V^T + \frac{D - D^T}{2} \tag{5.58}$$

is guaranteed to be asymptotically passive. This new model $H_{ap}(s)$ may exhibit a large deviation with respect to the original model response $H(s)$, since a constant term is added affecting the response at all frequencies. This accuracy loss can be partially compensated by a standard state-output matrix correction $\hat{C} = C + \delta C$, where δC is determined through

$$\min_{\delta C} \| \delta C \, (\jmath\omega I - A)^{-1}B + \hat{D} - D \|^2 \tag{5.59}$$

where the norm is defined, e. g., as a data-based cost function at discrete frequencies ω_ℓ, as in Section 5.4.2.

A second (preferable) approach for handling models that are not asymptotically passive amounts to:

1. Allowing for a perturbation of the direct coupling matrix $\hat{D} = D + \delta D$ in addition to the usual state-output map. The model perturbation thus becomes

$$\delta H(s) = \delta C(sI - A)^{-1}B + \delta D = \begin{pmatrix} \delta C & \delta D \end{pmatrix} \begin{pmatrix} (sI - A)^{-1}B \\ I \end{pmatrix} \tag{5.60}$$

   which is compatible with all previous derivations with obvious modifications. Note that, in this case, the Gramian-based cost functions become ill-defined since the L_2 norm of $\delta H(s)$ is not finite, and a data-based cost function over a limited bandwidth, such as (5.32), should be used during passivity enforcement.
2. Including an explicit local passivity constraint at $\omega = \infty$ during passivity enforcement. This constraint is just a simple particular case of (5.52), where $\delta D + \delta D^T$ replaces $\delta\Psi(\jmath\underline{\omega}_{kv})$.

We leave details of the above generalization to the reader.

5.6.3 Descriptor systems

Many model order reduction methods lead to systems in descriptor form

$$S: \quad \begin{cases} E\dot{x}(t) = Ax(t) + Bu(t), \\ y(t) = Cx(t) + Du(t), \end{cases} \tag{5.61}$$

with a possibly singular matrix E, and often with $D = 0$, instead of the regular state-space form (5.1). A fundamental requirement to avoid an ill-defined (non-solvable) model is that the pencil (A, E) is regular with $|sE - A| \neq 0$ for some $s \in \mathbb{C}$. In the following, we only discuss the case of *impulse-free* or equivalently *index-one* systems, for which the transfer function

$$H(s) = C(sE - A)^{-1}B + D \tag{5.62}$$

has a finite asymptotic value $H_\infty = \lim_{s\to\infty} H(s)$. Descriptor systems with higher index require a special treatment[7] which is outside the scope of this chapter. See [58, 84, 91, 96, 98] for details.

---

7 Index-two systems can be passive with a positive real transfer funciton $H(s)$ only when the leading asymptotic term $H(s) \sim sL_\infty$ for $s \to \infty$ is such that $L_\infty = L_\infty^T \geq 0$. Higher index systems are not passive and, in order to recover passivity, the high order impulsive part must be deflated.

For index-one descriptor systems the Hamiltonian-based passivity check is applicable with a minimal modification [91, 96, 98]. In fact, repeating the derivations of Sections 5.2.1.3 and 5.6.1 while using (5.61) as a starting point leads to the same generalized eigenvalue problem (5.56), but with $\mathcal{N}$ redefined as

$$\mathcal{N} = \begin{pmatrix} E & 0 & 0 \\ 0 & E^T & 0 \\ 0 & 0 & 0 \end{pmatrix}. \tag{5.63}$$

Special care should be taken in the (generalized) Hamiltonian eigenvalue computation, for which structured eigensolvers should be preferred to general-purpose eigensolvers; see e. g. the implicitly restarted Krylov method of [59].

Passivity enforcement of descriptor systems via Hamiltonian eigenvalue perturbation is discussed in [83, 84, 91, 96, 97, 98] and further generalized to para-Hermitian pencils in [16]. The Gramian-based cost function for minimizing model perturbation of Section 5.4.1 should also be properly generalized; see [78, 84] and [5, Chapter 2] for details. Finally, we refer the reader to [30] for an extension of the Positive Real Lemma to descriptor systems.

5.6.4 Other supply rates

All above derivations and algorithms assume that the supply rate $\mathsf{s}(u, y)$ through which power is delivered to the system from the environment is given by (5.7). However, this is not the only possible choice in general application fields. We review below the notable cases of scattering representations and general quadratic supply rates, discussing the various modifications that are required to define, check, and enforce passivity.

5.6.4.1 Scattering representations and bounded realness

The scattering representation is the most appropriate description of models in several application fields, in particular high-frequency electronics and electromagnetics. This is due to a number of reasons, including regularity and boundedness of the transfer function, as well as the ability to measure it with high accuracy. In scattering representations, the inputs u and outputs y are related to the power flow that is incident and reflected by the structure. In particular, the supply rate is defined as

$$\mathsf{s}(u, y) = u^T u - y^T y = \|u\|^2 - \|y\|^2 \tag{5.64}$$

and is interpreted as the net power transferred to the system from the environment, with the term $\|u\|^2$ denoting the power flow incident into the system and $\|y\|^2$ the corresponding power flow that is reflected or scattered back into the environment [2, 4, 90].

The supply rate $\mathsf{s}(u, y)$ in (5.64) leads to a set of passivity[8] conditions that are listed below, and which are obtained by repeating the derivations of Section 5.2.1 while applying the appropriate modifications.

The KYP Lemma for scattering representation is known as *Bounded Real Lemma (BRL)* [2, 74] and states that a scattering state-space system (5.1) is passive if and only if

$$\exists P = P^T > 0 : \quad \begin{pmatrix} A^T P + PA + C^T C & PB + C^T D \\ B^T P + D^T C & -(I - D^T D) \end{pmatrix} \leq 0. \tag{5.65}$$

This lemma can also be stated in the equivalent LMI form

$$\exists P = P^T > 0 : \quad \begin{pmatrix} A^T P + PA & PB & C^T \\ B^T P & -I & D^T \\ C & D & -I \end{pmatrix} \leq 0. \tag{5.66}$$

A scattering system is passive when its transfer function $H(s)$ is *Bounded Real (BR)*, i. e., the following three conditions hold [2, 81, 90]:

1. $H(s)$ must be regular in the open right half complex plane $\Re\{s\} > 0$;
2. $H(s^*) = H^*(s)$;
3. $\Psi(s) = I - H^T(-s)H(s) \geq 0$ for $\Re\{s\} > 0$.

These conditions should be compared to the PR conditions of Section 5.2.1.2, noting that the only difference between PR and BR is in the definition of the function $\Psi(s)$. Correspondingly, the frequency-domain inequality conditions for the passivity of a scattering system still require $\Psi(\jmath\omega) \geq 0$ for all $\omega \in \mathbb{R}$, and can be expressed as in (5.12). An equivalent statement is based on the singular values of the transfer function

$$\sigma_i \leq 1, \quad \forall \sigma_i \in \sigma\big(H(\jmath\omega)\big), \quad \forall \omega \in \mathbb{R}, \tag{5.67}$$

which implies in turn that passive scattering models must have a bounded and regular transfer function $H(s)$ when restricted to the imaginary axis $s = \jmath\omega$, further requiring that the state-space matrix A must be asymptotically stable. Another yet equivalent condition for passivity is expressed in terms of the superior of the largest singular value throughout the imaginary axis, leading to the well-known $\mathcal{H}_\infty$ norm condition

$$\|H\|_{\mathcal{H}_\infty} = \sup_{\omega \in \mathbb{R}} \sigma_{\max}\big(H(\jmath\omega)\big) \leq 1. \tag{5.68}$$

The Hamiltonian matrix associated to a scattering state-space system (5.1) reads

$$\mathcal{M} = \begin{pmatrix} A - B(I - D^T D)^{-1} D^T C & -B(I - D^T D)^{-1} B^T \\ C^T (I - DD^T)^{-1} C & -A^T + C^T D (I - D^T D)^{-1} B^T \end{pmatrix}. \tag{5.69}$$

8 We retain the general term *passivity* also in the scattering (and for general quadratic supply rates), as a standard denomination in circuit, electronic and electromagnetic applications, although in some scientific communities this term is dedicated to immittance representations, and the term *dissipative* is used in the more general setting.

The system is passive if $\mathcal{M}$ has no purely imaginary eigenvalues (strictly passive) or at most purely imaginary eigenvalues with even-sized Jordan blocks [12, 33]. The same considerations of Section 5.2.1.3 apply. When the model is not asymptotically passive for $\omega \to \infty$, then D has one unit singular value and the above Hamiltonian matrix becomes ill-defined. In this case, $\mathcal{M}$ generalizes to the pencil $(\mathcal{M}, \mathcal{N})$ where

$$\mathcal{M} = \begin{pmatrix} A & 0 & B & 0 \\ 0 & -A^T & 0 & -C^T \\ 0 & B^T & -I & D^T \\ C & 0 & D & -I \end{pmatrix}, \quad \mathcal{N} = \begin{pmatrix} I & 0 & 0 & 0 \\ 0 & I & 0 & 0 \\ 0 & 0 & 0 & 0 \\ 0 & 0 & 0 & 0 \end{pmatrix} \tag{5.70}$$

which replaces (5.56) for scattering representations [91, 94, 97, 98]. Finally, when the underlying system is in descriptor form (5.61), then we simply replace I with E in $\mathcal{N}$, as in (5.63).

With all above redefinitions of appropriate passivity conditions for scattering systems, all passivity check and enforcement algorithms discussed in Section 5.3 and Section 5.5 apply with obvious modifications.

5.6.4.2 General quadratic supply rates

Immittance and scattering representations are just particular cases of the more general situation in which the supply rate is a quadratic function of input and output variables. Such case is compactly described by

$$\mathsf{s}(u, y) = \begin{pmatrix} u \\ y \end{pmatrix}^T \begin{pmatrix} Q & S \\ S^T & R \end{pmatrix} \begin{pmatrix} u \\ y \end{pmatrix} \tag{5.71}$$

with $Q = Q^T$ and $R = R^T$, from which the immittance case (5.7) and the scattering case (5.64) are obtained by setting $Q = R = 0$, $S = I$ (up to the irrelevant scaling factor 1/2) and $Q = I$, $R = -I$, $S = 0$, respectively.

The LMI condition (KYP lemma) that characterizes a passive (dissipative) state-space system (5.1) with supply rate (5.71) reads

$$\exists P = P^T > 0 : \quad \begin{pmatrix} A^T P + PA - C^T RC & PB - (SC)^T - C^T RD \\ B^T P - SC - D^T RC & -Q - SD - (SD)^T - D^T RD \end{pmatrix} \leq 0, \tag{5.72}$$

and the corresponding Frequency-Domain Inequality reads

$$\Psi(\jmath\omega) = Q + H^H(\jmath\omega)S^T + SH(\jmath\omega) + H^H(\jmath\omega)RH(\jmath\omega) \geq 0, \quad \forall \omega \in \mathbb{R}. \tag{5.73}$$

Finally, the Hamiltonian matrix that generalizes (5.16) and (5.69) reads

$$\mathcal{M} = \begin{pmatrix} A - BW^{-1}Z & -BW^{-1}B^T \\ -C^T RC + Z^T W^{-1} Z & -A^T + Z^T W^{-1} B^T \end{pmatrix} \tag{5.74}$$

where $W = Q + SD + (SD)^T + D^T RD$ and $Z = (SC + D^T RC)$. We leave all details to the reader, pointing to [74, 88, 89] for a complete theoretical discussion. With suitable

modifications, all passivity verification and enforcement schemes of Section 5.3 and Section 5.5 are applicable to this general case as well.

5.6.5 Enforcing stability

All results and algorithms presented up to now are based on the fundamental assumption that the system at hand is asymptotically stable, with all eigenvalues of state matrix A, or pencil (A, E) in the descriptor case, having a strictly negative real part. Many MOR schemes are able to preserve stability if the original model is stable, for instance balanced truncation [5, Chapter 2] or Krylov subspace methods based on split congruence transformations such as PRIMA [6, Chapter 4]. Basic Arnoldi or Lanczos methods are instead not generally able to preserve stability in the reduced order model. Considering data-driven methods, the Vector Fitting algorithm [5, Chapter 8] incorporates a pole-flipping strategy that guarantees stability, whereas basic Loewner interpolation/reduction schemes [5, Chapter 6] do not guarantee stability. Further, even if a stability-preserving MOR method is used, roundoff errors in computer implementations may compromise the stability and may result in some eigenvalue with a positive real part.

Stabilization of a given model or system is a standard problem in Control Theory, where many alternative approaches usually based on feedback are routinely applied. The Reader is referred to any textbook such as [99]. The requirements we have in MOR applications are stronger than simple stabilization, since the final model should be as close as possible to the initial (unstable) model according to a prescribed performance metric or norm. Therefore, the simplistic approach of separating the unstable modes through an eigenvalue or, better, Schur decomposition and simply discarding them is not appropriate. Optimal stabilizing approximations are in fact available through robust and reliable algorithms. As an example, we refer the reader to [52], where some approaches for finding the closest stable system based on $\mathcal{H}_2$ and $\mathcal{H}_\infty$ norms are introduced; see also [32].

5.6.6 Parameterized systems

Passivity verification and enforcement methods can be extended to parameterized systems, whose response $H(s, \vartheta)$ depends both on frequency s and (multivariate) parameters $\vartheta \in \Theta \subseteq \mathbb{R}^d$. In this framework, many different approaches and solutions have been proposed, depending on how parameters are embedded in the model and on how the model is constructed. A complete treatment would be outside the scope of this chapter, so that we discuss only a specific yet wide class of model parameterizations

$$H(s;\vartheta) = \frac{\mathsf{N}(s,\vartheta)}{\mathsf{D}(s,\vartheta)} = \frac{\sum_{n=0}^{\bar{n}} \sum_{\ell=1}^{\bar{\ell}} R_{n,\ell}\, \xi_\ell(\vartheta)\, \varphi_n(s)}{\sum_{n=0}^{\bar{n}} \sum_{\ell=1}^{\bar{\ell}} r_{n,\ell}\, \xi_\ell(\vartheta)\, \varphi_n(s)}, \tag{5.75}$$

where $R_{n,\ell} \in \mathbb{R}^{M\times M}$ and $r_{n,\ell} \in \mathbb{R}$ are the model coefficients, $\varphi_n(s)$, $\xi_\ell(\vartheta)$ are suitable basis functions representing the dependence of model numerator and denominator on frequency and parameters, respectively, and ℓ is a scalar index spanning the parameter basis set through a suitable linear ordering. The parameterization (5.75) includes as particular cases the multivariate barycentric form leading to the (parameterized) Loewner framework [50] (see [5, Chapter 6]) and the generalized Sanathanan–Koerner form [38, 80], which extends to the multivariate setting the Vector Fitting scheme [5, Chapter 8]. In the latter case the frequency basis functions are $\varphi_0(s) = 1$ and $\varphi_n(s) = (s - q_n)^{-1}$ for $n > 0$, where q_n are predefined stable "basis poles", either real or in complex conjugate pairs, and the parameter-dependent basis functions ξ_ℓ can be orthogonal or trigonometric polynomials, or any other choice that is appropriate for the application at hand. A parameterized (descriptor) realization is easily obtained from (5.75) as (5.61), where

$$A = A(\vartheta) = \sum_{\ell=1}^{\bar{\ell}} A_\ell \xi_\ell(\vartheta), \quad C = C(\vartheta) = \sum_{\ell=1}^{\bar{\ell}} C_\ell \xi_\ell(\vartheta) \tag{5.76}$$

and E, B, D are constant.

One notable and simple approach to obtain a uniformly passive model, so that all passivity conditions discussed in Section 5.2.1 hold $\forall \vartheta \in \Theta$, is to suppress the denominator in (5.75) as $\mathsf{D}(s) = 1$ and construct the parameterized system through interpolation of a set of non-parameterized models. This is achieved by choosing ξ_ℓ as interpolating, e. g. Lagrange, basis functions. There exist passivity-preserving interpolation schemes that ensure that, if the individual models being interpolated are passive, then also the interpolated parameterized model is passive $\forall \vartheta \in \Theta$. See [26, 27, 28, 29, 70] and the references therein for details on various alternative approaches within this framework.

A complementary approach is to consider the fully-parameterized model in form (5.75) and extend the passivity verification and enforcement methods of Section 5.3 and Section 5.5 to the multivariate case. The main difficulty that arises in this scenario is that the Hamiltonian matrix, which is the main tool providing localization of the passivity violations, becomes parameter-dependent due to (5.76). The convenience of the purely algebraic test based on its eigenvalues is partially lost, since the purely imaginary eigenvalues (if any) are parameter-dependent. A possible strategy for tracking these eigenvalues based on adaptive sampling in the parameter space is discussed in [95], where a first-order perturbation analysis on the full Hamiltonian eigenspectrum is used to determine the regions in the parameter space that need refined sampling, in order to track the boundaries between the regions defining passive and non-passive models. Figure 5.5 provides an illustration by depicting the results of this adaptive sampling process in a case with two parameters $d = 2$. If any passivity violation region is detected (the red dots in Figure 5.5, left panel), then the worst-case passivity violations are determined as in Algorithm 5.1 and a multivariate extension of Algorithm 5.3 is applied to eliminate them. All details are available in [37, 40, 95].

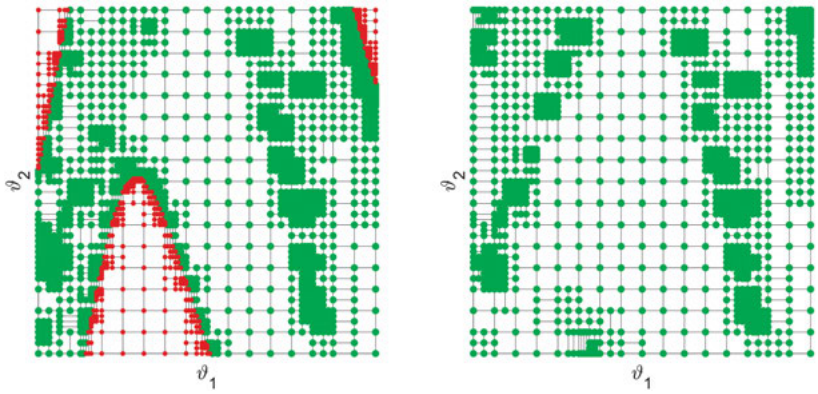

Figure 5.5: Adaptive sampling in a two-dimensional parameter space, applied to a non-passive model (left panel) and to the corresponding passive model after enforcement (right). Each dot represents a non-parameterized model instance obtained by evaluating the parameterized model (5.75) at the corresponding sampling point. Each dot is colored in green/red if the corresponding model instance is locally passive/non-passive, respectively, as resulting from the absence/presence of imaginary Hamiltonian eigenvalues. Iterative refinement leads to tracking the boundaries between passive/non-passive regions. Courtesy of A. Zanco, Politecnico di Torino.

5.7 Examples

5.7.1 A high-speed interconnect in a mobile device

The passivity enforcement process is here applied to a model of a high-speed interconnect providing a data link in a smartphone. An initial characterization of the structure was obtained through a full-wave numerical simulation of the time-harmonic Maxwell's equations, which provided a set of frequency samples of the 4×4 (scattering) transfer function $S(\jmath\omega)$ from 0 to 50 GHz. These samples were processed by Vector Fitting [5, Chapter 8], obtaining a rational approximation of the system responses. This rational approximation was then converted to a state-space realization as in [5, Chapter 8]. The accuracy of the rational approximation is excellent, as depicted in the two top panels of Figure 5.6.

A Hamiltonian-based passivity check on this model reveals the presence of $K = 10$ purely imaginary Hamiltonian eigenvalues $\mu_k = \jmath\omega_k$ (see Figure 5.7, left panel). Correspondingly, a sweep of the model singular values $\sigma_i(H(\jmath\omega))$ (see the top panel of Figure 5.8) up to a maximum frequency slightly beyond ω_K reveals a few evident passivity violations, corresponding to singular value trajectories exceeding the passivity threshold $\sigma = 1$. The local singular value maxima are highlighted with red dots in Figure 5.8.

Figure 5.8 depicts the typical situation that arises when fitting a rational model to response data over a finite frequency band: passivity violations usually occur at frequencies that fall outside the range where data samples are available. The fact that

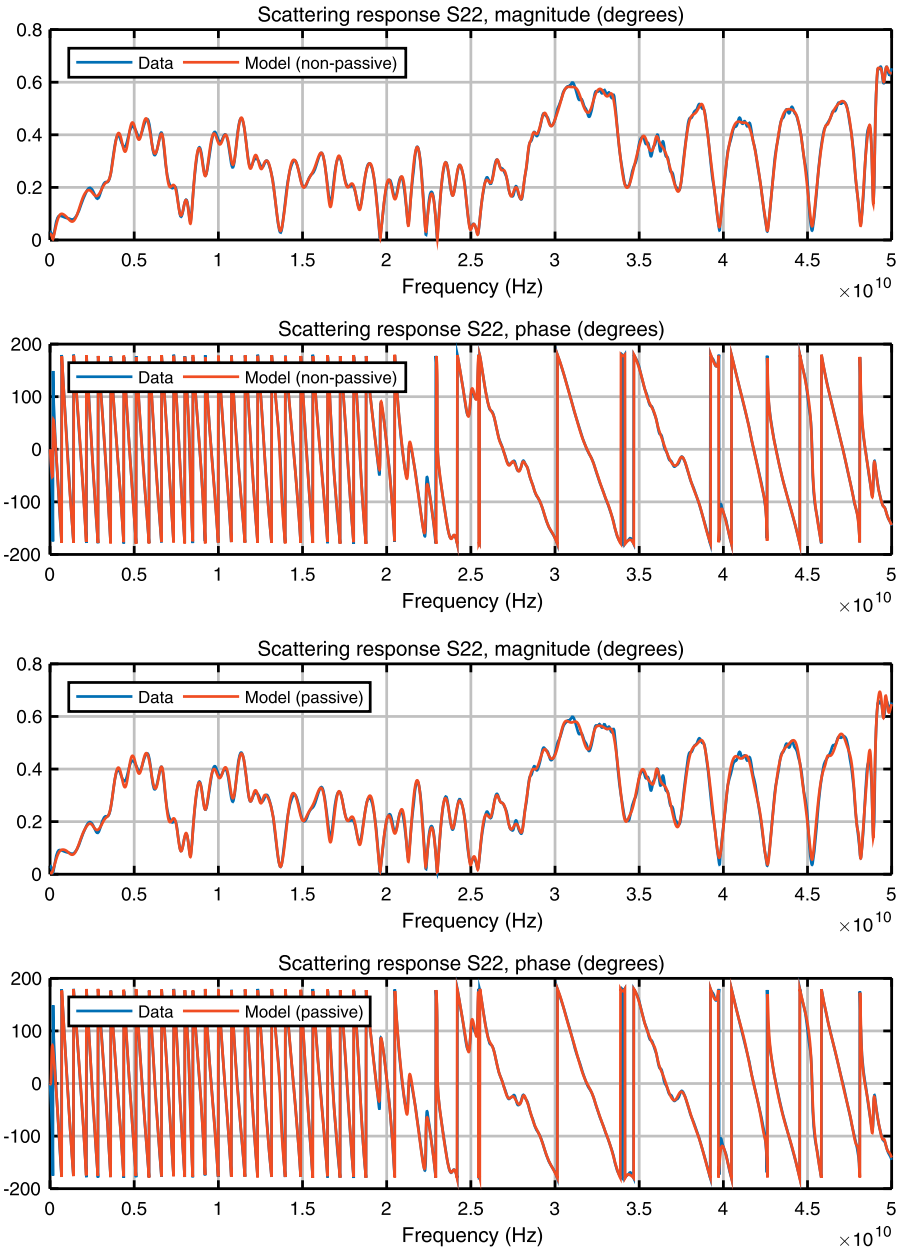

Figure 5.6: Comparison between model and original data used for model extraction for the smartphone interconnect. For illustration, only response $S_{22}(\jmath\omega)$ of the 4×4 scattering matrix is reported. Top two panels refer to the initial non-passive model, whereas bottom two panels refer to the model after passivity enforcement.

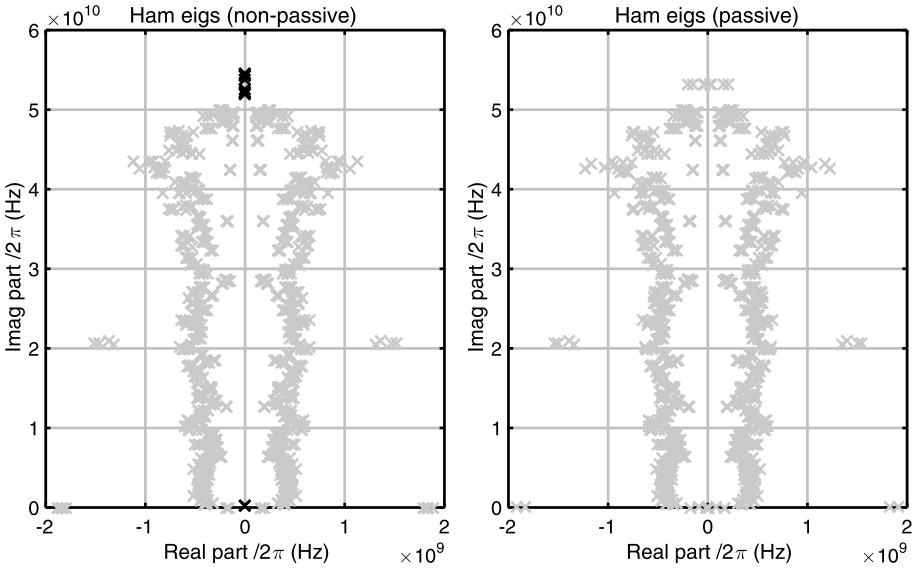

Figure 5.7: Hamiltonian eigenvalues before (left) and after (right) passivity enforcement for the smartphone interconnect model (only eigenvalues with positive imaginary parts are shown). The purely imaginary eigenvalues are highlighted with a darker color in the left panel.

such violations are not located within the modeling bandwidth may induce a false sense of confidence in the model user, who may argue that out-of-band passivity violations are unimportant, since located at frequency ranges that are not of interest. In fact, a time-domain simulation of the model using a transient ODE solver is agnostic whether the passivity violation occurs within or off-band: during time-stepping, numerical approximation errors due to the adopted ODE solver will inevitably excite those frequencies where the model amplifies energy, leading to instability. This is exactly what happens in Figure 5.1, where the thin blue line demonstrates the instability induced by this initial non-passive model. In this simulation scenario, the model was interconnected to a set of other linear (passive) circuits, and it was indeed possible to determine exactly the two poles $p = 2\pi(\alpha \pm \jmath\beta)$ that are responsible for this instability, obtaining $\alpha = +1.13 \times 10^8$ Hz and $\beta = 5.32 \times 10^{10}$ Hz. The real part is positive, and the imaginary part nearly matches the frequency of the singular value peak; see Figure 5.8. This is exactly the frequency where the model injects energy into the system. See [35] for additional details on destabilization of non-passive models.

Enforcing model passivity removes the instability, as we already know from Figure 5.1. Application of Algorithm 5.3 leads to a passive model in 5 iterations, documented by the singular value plots in the various panels of Figure 5.8. The final passive model has no purely imaginary Hamiltonian eigenvalues, as evident from the right panel of Figure 5.7, and its responses still match very accurately the original data samples, as depicted in the bottom panel of Figure 5.6.

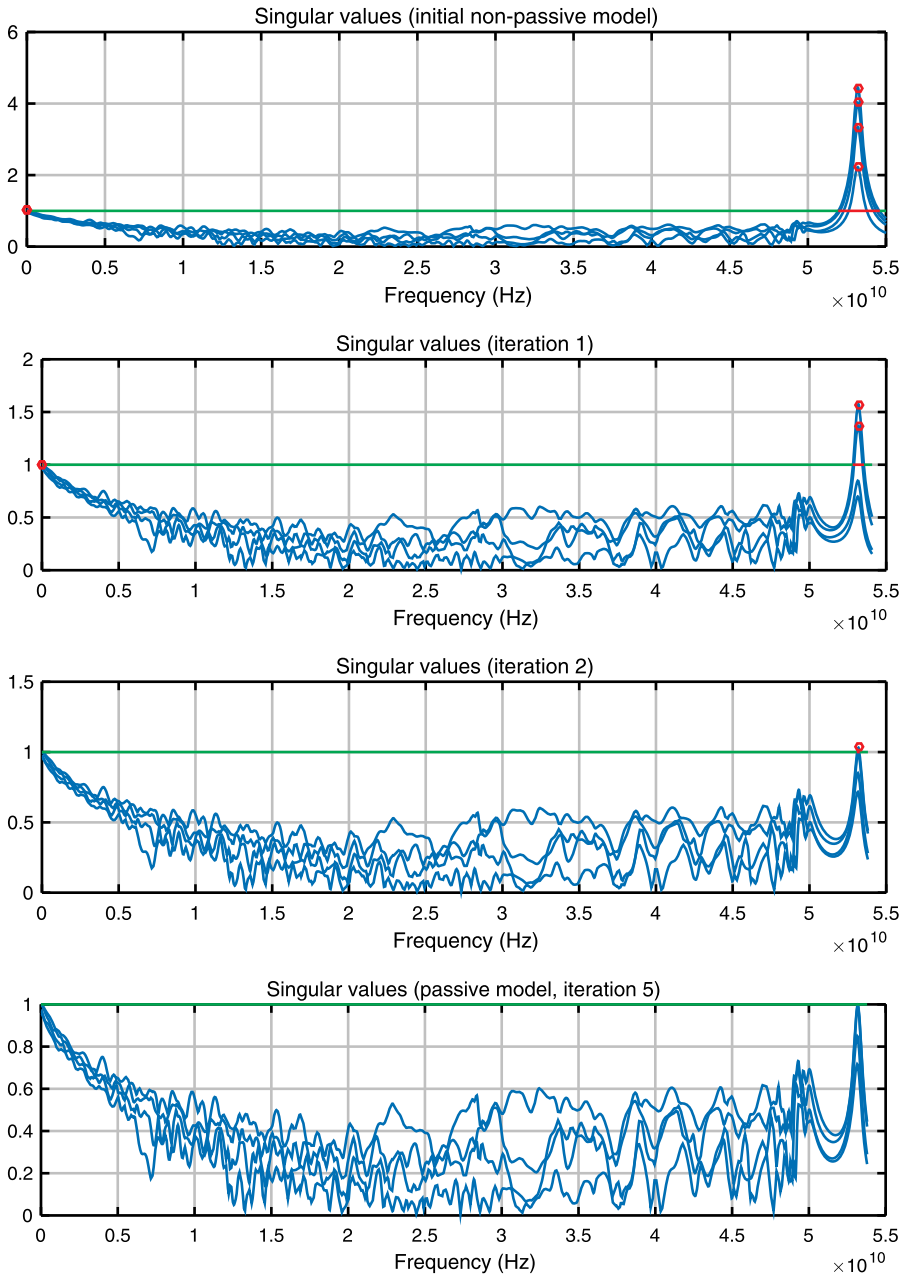

Figure 5.8: Evolution of the singular values (blue solid lines) of the smartphone interconnect during passivity enforcement iterations through Algorithm 5.3. Passive and non-passive frequency bands are highlighted with green and red color, respectively. Local maxima of all singular value trajectories in each non-passive frequency band, which are used to set up local passivity constraints, are highlighted with red dots.

5.7.2 An interconnect link on a high-performance PCB

We consider here the coupled interconnect link on a high-performance Printed Circuit Board (PCB), already discussed in [5, Chapter 8], where an accurate model was extracted using the Vector Fitting algorithm from scattering measurements performed on the real hardware. As depicted in [5, Chapter 8], Figures 6 and 7, the model responses of this initial model are visually undistinguishable from the measured samples, with a model-data error of $1.34 \cdot 10^{-3}$ (worst-case RMS error among all responses).

A passivity check performed on this initial model reveals some small passivity violations at low frequencies. This is actually expected, since the system is almost lossless at low frequency, and passivity violations induced by the rational approximation process of VF are therefore more likely than at high frequency, where energy dissipation is more pronounced. The passivity violations are detected by the presence of eight pairs of purely imaginary Hamiltonian eigenvalues, depicted in Figure 5.9, panels (a), (c) and (d). The corresponding frequencies denote crossings of the singular

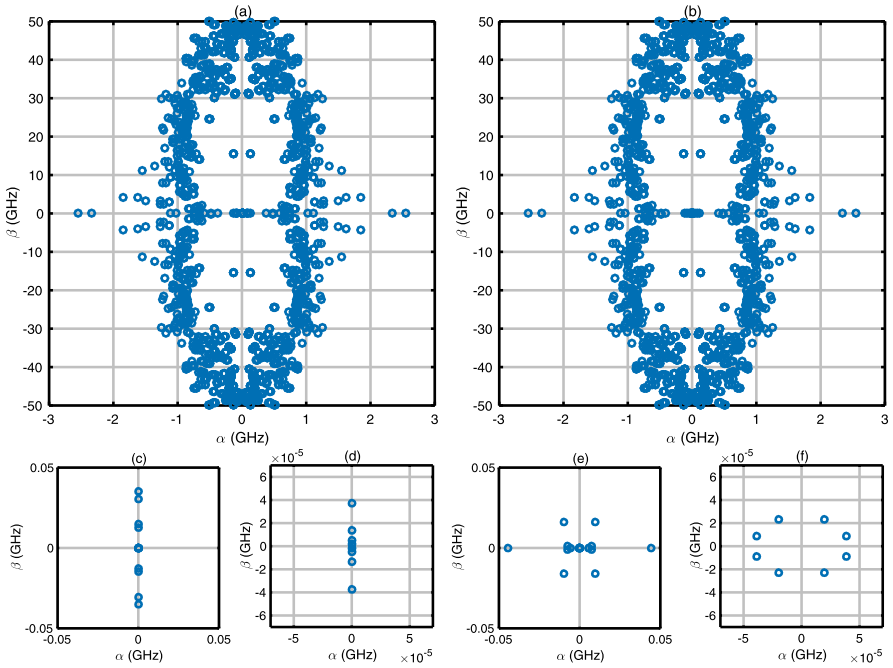

Figure 5.9: Hamiltonian eigenvalues $\alpha + j\beta = \mu/2\pi$ of the PCB interconnect model. Panels (a), (c), (d): original model after Vector Fitting; panels (b), (e), (f): model after passivity enforcement. Top panels (a), (b) depict the full Hamiltonian eigenspectrum. Bottom panels (c), (d) and (e), (f) are enlarged views of the top panels (a) and (b), respectively, at different magnification levels. Panels (e) and (f) show that all purely imaginary Hamiltonian eigenvalues clustered at low frequencies, depicted in panels (c) and (d), are effectively removed by passivity enforcement.

value trajectories $\sigma_i(\jmath\omega)$ of the threshold $\sigma = 1$, as depicted in Figure 5.10, top panel. After few iterations of Algorithm 5.3 all these passivity violations are removed. As the bottom panel of Figure 5.10 shows, all singular value trajectories of the passive model are uniformly bounded by one. This is further confirmed by panels (e) and (f) of Figure 5.9, which show that all purely imaginary eigenvalues of the initial model are now displaced from the imaginary axis.

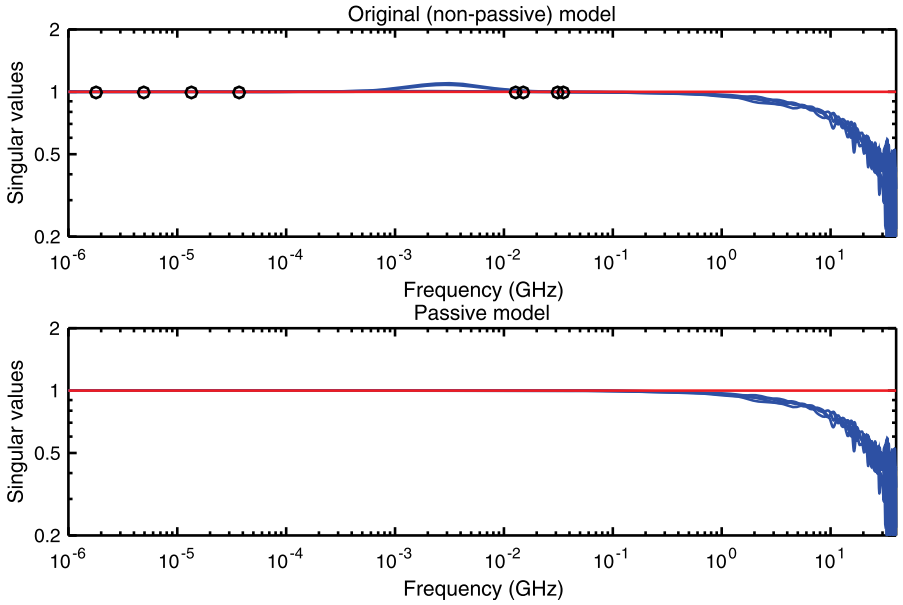

Figure 5.10: Top panel: singular value trajectories (blue lines) of the initial (non-passive) PCB interconnect model, revealing low-frequency passivity violations exceeding the passivity threshold $\sigma = 1$ (red line). Black dots correspond to the frequencies of the purely imaginary Hamiltonian eigenvalues; see Figure 5.9, panels (c) and (d). Bottom panel: singular value trajectories after passivity enforcement, which are uniformly below the passivity threshold.

The passivity enforcement process did not spoil model accuracy. Figure 5.11 compares the scattering responses $(1, 2)$ and $(1, 3)$ of the passive model to the raw measured samples from which the initial model was derived (the same responses already depicted in [5, Chapter 8], Figures 6 and 7). Also for the passive model the responses closely match the measurements, with a worst-case RMS model-data error of $1.38 \cdot 10^{-3}$.

5.8 Conclusions

The goal of this chapter was to survey the most widely used techniques for enforcing passivity of reduced order models. To motivate the ensuing description, a simple

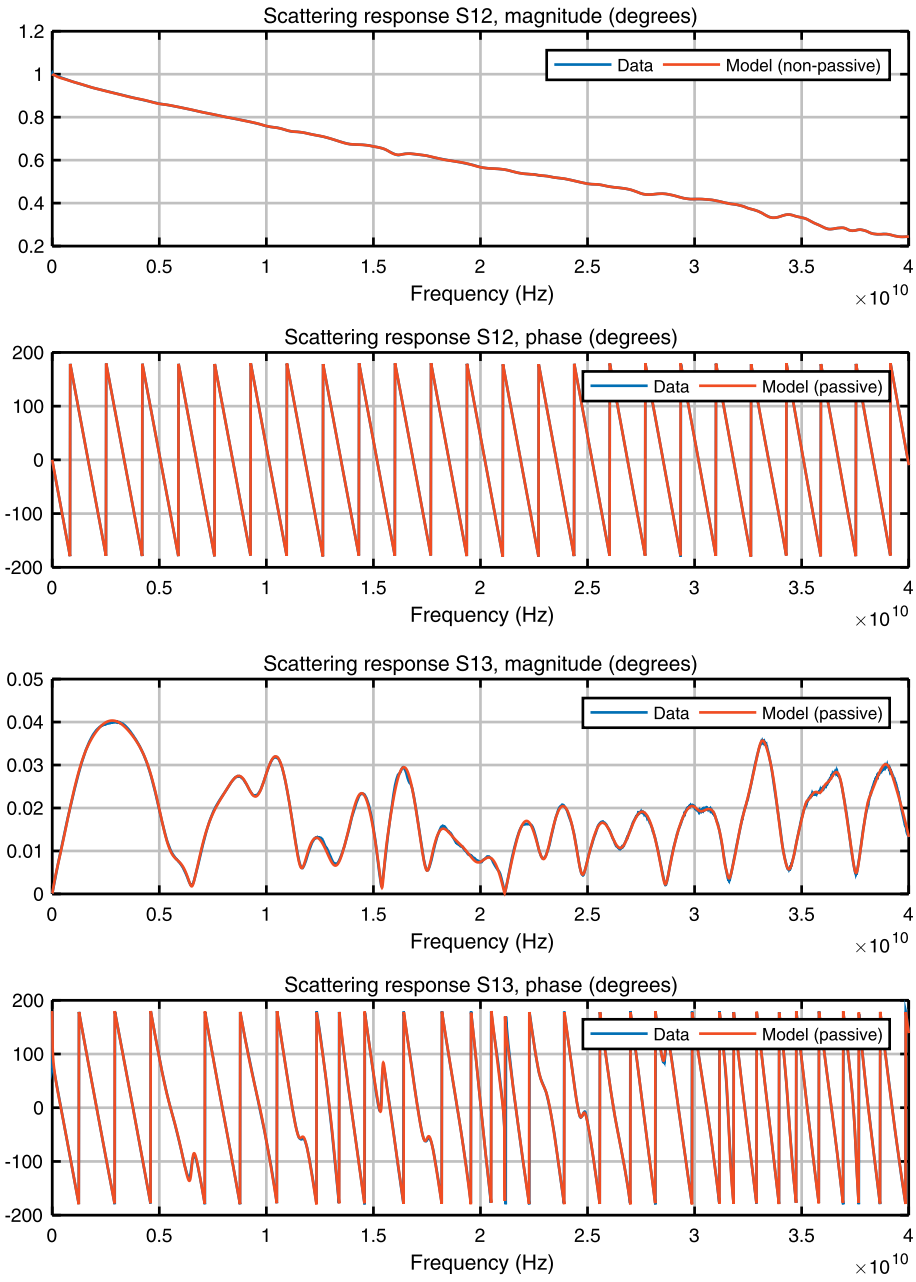

Figure 5.11: Comparison between passive model responses and measured data used for model identification for the high-speed PCB interconnect of Section 5.7.2.

example was shown that illustrates in striking fashion the need for ensuring passivity in models. The focus of the chapter was on Linear Time-Invariant (LTI) systems in state-space form, although the techniques reviewed are applicable in other representations with appropriate modifications. Conditions for testing the passivity of a given LTI model as well as approaches for perturbing non-passive systems in order to enforce passivity were reviewed and examples were shown to demonstrate the application of such techniques to realistic cases.

Bibliography

[1] R. Alam, S. Bora, M. Karow, V. Mehrmann, and J. Moro. Perturbation theory for Hamiltonian matrices and the distance to bounded-realness. *SIAM J. Matrix Anal. Appl.*, 32(2):484–514, 2011.

[2] B. D. O. Anderson and S. Vongpanitlerd. *Network analysis and synthesis*. Prentice-Hall, 1973.

[3] Z. Bai, J. Demmel, J. Dongarra, A. Ruhe and H. van der Vorst. *Templates for the solution of Algebraic Eigenvalue Problems: A Practical Guide*. Society for Industrial and Applied Mathematics, 2000.

[4] V. Belevitch. *Classical network theory*. Holden-Day, 1968.

[5] P. Benner, S. Grivet-Talocia, A. Quarteroni, G. Rozza, W. Schilders and L. Silveira. *Model Order Reduction. Volume 1: System- and Data-Driven Methods and Algorithms*. De Gruyter, Berlin, 2020.

[6] P. Benner, S. Grivet-Talocia, A. Quarteroni, G. Rozza, W. Schilders and L. Silveira. *Model Order Reduction. Volume 3: Applications*. De Gruyter, Berlin, 2020.

[7] P. Benner and D. Kressner. Algorithm 854: Fortran 77 subroutines for computing the eigenvalues of Hamiltonian matrices II. *ACM Trans. Math. Softw.*, 32(2):352–373, 2006.

[8] P. Benner and D. Kressner. Balancing sparse Hamiltonian eigenproblems. *Linear Algebra Appl.*, 415(1):3–19, 2006. Special Issue on Large Scale Linear and Nonlinear Eigenvalue Problems.

[9] P. Benner, D. Kressner, and V. Mehrmann. Skew-Hamiltonian and Hamiltonian eigenvalue problems: Theory, algorithms and applications. In Z. Drmac, M. Marusic and Z. Tutek, editors, *Proceedings of the Conference on Applied Mathematics and Scientific Computing*, pages 3–39. Springer, Netherlands, 2005.

[10] P. Benner, V. Mehrmann, V. Sima, S. Huffel, and A. Varga. SLICOT–a subroutine library in systems and control theory. In B. Datta, editor, *Applied and Computational Control, Signals, and Circuits*, pages 499–539. Birkhäuser, Boston, 1999.

[11] P. Benner and M. Voigt. Spectral characterization and enforcement of negative imaginariness for descriptor systems. *Linear Algebra Appl.*, 439(4):1104–1129, 2013. 17th Conference of the International Linear Algebra Society, Braunschweig, Germany, August 2011.

[12] S. Boyd, V. Balakrishnan, and P. Kabamba. A bisection method for computing the H_∞ norm of a transfer matrix and related problems. *Math. Control Signals Syst.*, 2(3):207–219, 1989.

[13] S. Boyd, L. El Ghaoui, E. Feron, and V. Balakrishnan. *Linear matrix inequalities in system and control theory*, volume 15. Society for Industrial and Applied Mathematics, 1994.

[14] S. P. Boyd and L. Vandenberghe. *Convex optimization*. Cambridge University Press, 2004.

[15] B. Brogliato, R. Lozano, B. Maschke, and O. Egeland. *Dissipative systems analysis and control: theory and applications*. Springer, 2007.

[16] T. Brull and C. Schroder. Dissipativity enforcement via perturbation of para-Hermitian pencils. *IEEE Trans. Circuits Syst. I, Regul. Pap.*, 60(1):164–177, 2013.

[17] A. Buscarino, L. Fortuna, M. Frasca, and M. G. Xibilia. An analytical approach to one-parameter MIMO systems passivity enforcement. *Int. J. Control*, 85(9):1235–1247, 2012.

[18] H. Chen and J. Fang. Enforcing bounded realness of S parameter through trace parameterization. In *Electrical Performance of Electronic Packaging, 2003*, pages 291–294, 2003.

[19] X. Chen and J. T. Wen. Positive realness preserving model reduction with H_∞ norm error bounds. *IEEE Trans. Circuits Syst. I, Fundam. Theory Appl.*, 42(1):23–29, 1995.

[20] A. Chinea, S. Grivet-Talocia, S. B. Olivadese, and L. Gobbato. High-performance passive macromodeling algorithms for parallel computing platforms. *IEEE Trans. Compon. Packag. Manuf. Technol.*, 3(7):1188–1203, 2013.

[21] C. P. Coelho, J. Phillips, and L. M. Silveira. A convex programming approach for generating guaranteed passive approximations to tabulated frequency-data. *IEEE Trans. Comput.-Aided Des. Integr. Circuits Syst.*, 23(2):293–301, 2004.

[22] D. Deschrijver and T. Dhaene. Fast passivity enforcement of S-parameter macromodels by pole perturbation. *IEEE Trans. Microw. Theory Tech.*, 57(3):620–626, 2009.

[23] D. Deschrijver and T. Dhaene. Modified half-size test matrix for robust passivity assessment of S-parameter macromodels. *IEEE Microw. Wirel. Compon. Lett.*, 19(5):263–265, 2009.

[24] C. A. Desoer and E. S. Kuh. *Basic circuit theory*. McGraw-Hill, 1984.

[25] B. Dumitrescu. Parameterization of positive-real transfer functions with fixed poles. *IEEE Trans. Circuits Syst. I, Fundam. Theory Appl.*, 49(4):523–526, 2002.

[26] F. Ferranti, T. Dhaene, and L. Knockaert. Compact and passive parametric macromodeling using reference macromodels and positive interpolation operators. *IEEE Trans. Compon. Packag. Manuf. Technol.*, 2(12):2080–2088, 2012.

[27] F. Ferranti, L. Knockaert, and T. Dhaene. Parameterized S-parameter based macromodeling with guaranteed passivity. *IEEE Microw. Wirel. Compon. Lett.*, 19(10):608–610, 2009.

[28] F. Ferranti, L. Knockaert, and T. Dhaene. Guaranteed passive parameterized admittance-based macromodeling. *IEEE Trans. Adv. Packaging*, 33(3):623–629, 2010.

[29] F. Ferranti, L. Knockaert, T. Dhaene, G. Antonini, and D. De Zutter. Parametric macromodeling for tabulated data based on internal passivity. *IEEE Microw. Wirel. Compon. Lett.*, 20(10):533–535, 2010.

[30] R. W. Freund and F. Jarre. An extension of the positive real lemma to descriptor systems. *Optim. Methods Softw.*, 19(1):69–87, 2004.

[31] S. Gao, Y.-S. Li, and M.-S. Zhang. An efficient algebraic method for the passivity enforcement of macromodels. *IEEE Trans. Microw. Theory Tech.*, 58(7):1830–1839, 2010.

[32] I. V. Gosea and A. C. Antoulas. Stability preserving post-processing methods applied in the Loewner framework. In *2016 IEEE 20th Workshop on Signal and Power Integrity (SPI)*, pages 1–4, 2016.

[33] S. Grivet-Talocia. Passivity enforcement via perturbation of Hamiltonian matrices. *IEEE Trans. Circuits Syst. I, Fundam. Theory Appl.*, 51(9):1755–1769, 2004.

[34] S. Grivet-Talocia. An adaptive sampling technique for passivity characterization and enforcement of large interconnect macromodels. *IEEE Trans. Adv. Packaging*, 30(2):226–237, 2007.

[35] S. Grivet-Talocia. On driving non-passive macromodels to instability. *Int. J. Circuit Theory Appl.*, 37(8):863–886, 2009.

[36] S. Grivet-Talocia. On passivity characterization of symmetric rational macromodels. *IEEE Trans. Microw. Theory Tech.*, 58(5):1238–1247, 2010.

[37] S. Grivet-Talocia. A perturbation scheme for passivity verification and enforcement of parameterized macromodels. *IEEE Trans. Compon. Packag. Manuf. Technol.*, 7(11):1869–1881, 2017.

[38] S. Grivet-Talocia and E. Fevola. Compact parameterized black-box modeling via Fourier-rational approximations. *IEEE Trans. Electromagn. Compat.*, 59(4):1133–1142, 2017.
[39] S. Grivet-Talocia and B. Gustavsen. *Passive Macromodeling: Theory and Applications*. John Wiley and Sons, New York, 2016 (published online on Dec 7, 2015).
[40] S. Grivet-Talocia and R. Trinchero. Behavioral, parameterized, and broadband modeling of wired interconnects with internal discontinuities. *IEEE Trans. Electromagn. Compat.*, 60(1):77–85, 2018.
[41] S. Grivet-Talocia and A. Ubolli. On the generation of large passive macromodels for complex interconnect structures. *IEEE Trans. Adv. Packaging*, 29(1):39–54, 2006.
[42] S. Grivet-Talocia and A. Ubolli. Passivity enforcement with relative error control. *IEEE Trans. Microw. Theory Tech.*, 55(11):2374–2383, 2007.
[43] S. Grivet-Talocia and A. Ubolli. A comparative study of passivity enforcement schemes for linear lumped macromodels. *IEEE Trans. Adv. Packaging*, 31(4):673–683, 2008.
[44] B. Gustavsen. Computer code for passivity enforcement of rational macromodels by residue perturbation. *IEEE Trans. Adv. Packaging*, 30(2):209–215, 2007.
[45] B. Gustavsen. Fast passivity enforcement for pole-residue models by perturbation of residue matrix eigenvalues. *IEEE Trans. Power Deliv.*, 23(4):2278–2285, 2008.
[46] B. Gustavsen and A. Semlyen. Enforcing passivity for admittance matrices approximated by rational functions. *IEEE Trans. Power Syst.*, 16(1):97–104, 2001.
[47] B. Gustavsen and A. Semlyen. Fast passivity assessment for S-parameter rational models via a half-size test matrix. *IEEE Trans. Microw. Theory Tech.*, 56(12):2701–2708, 2008.
[48] B. Gustavsen and A. Semlyen. On passivity tests for unsymmetrical models. *IEEE Trans. Power Deliv.*, 24(3):1739–1741, 2009.
[49] D. Henrion. Course on LMI optimization with applications in control, Czech Technical University, Prague, Czech Republic, April 2013. http://homepages.laas.fr/henrion/courses/lmi13/. Accessed: 2018-11-27.
[50] A. Ionita and A. Antoulas. Data-driven parametrized model reduction in the loewner framework. *SIAM J. Sci. Comput.*, 36(3):A984–A1007, 2014.
[51] R. E. Kalman. Lyapunov functions for the problem of Lur'e in automatic control. *Proc. Natl. Acad. Sci.*, 49(2):201–205, 1963.
[52] M. Köhler. On the closest stable descriptor system in the respective spaces RH_2 and RH_∞. *Linear Algebra Appl.*, 443:34–49, 2014.
[53] A. Lamecki and M. Mrozowski. Equivalent SPICE circuits with guaranteed passivity from nonpassive models. *IEEE Trans. Microw. Theory Tech.*, 55(3):526–532, 2007.
[54] P. Lancaster and L. Rodman. Existence and uniqueness theorems for the algebraic Riccati equation. *Int. J. Control*, 32(2):285–309, 1980.
[55] J. L. Yalmip. A toolbox for modeling and optimization in Matlab. In *Computer Aided Control Systems Design, 2004 IEEE International Symposium on*, pages 284–289. IEEE, 2004.
[56] A. I. Luré. Some Non-linear Problems in the Theory of Automatic Control: Nekotorye Nelineinye Zadachi Teorii Avtomaticheskogo Regulirovaniya (Gos. Isdat. Tekh. Teor. Lit., 1951, U. S. S. R.) A Translation from the Russian. H.M. Stationery Office, 1957.
[57] M. A. Mabrok, A. G. Kallapur, I. R. Petersen, and A. Lanzon. Enforcing a system model to be negative imaginary via perturbation of Hamiltonian matrices. In *Decision and Control and European Control Conference (CDC-ECC), 2011 50th IEEE Conference on*, pages 3748–3752, 2011.
[58] R. März. Canonical projectors for linear differential algebraic equations. *Comput. Math. Appl.*, 31(4–5):121–135, 1996. Selected Topics in Numerical Methods.
[59] V. Mehrmann, C. Schröder, and V. Simoncini. An implicitly-restarted Krylov subspace method for real symmetric/skew-symmetric eigenproblems. *Linear Algebra Appl.*, 436(10):4070–4087, 2012.

[60] V. Mehrmann and D. Watkins. Structure-preserving methods for computing eigenpairs of large sparse skew-Hamiltonian/Hamiltonian pencils. *SIAM J. Sci. Comput.*, 22(6):1905–1925, 2001.
[61] V. Mehrmann and H. Xu. Perturbation of purely imaginary eigenvalues of Hamiltonian matrices under structured perturbations. *Electron. J. Linear Algebra*, 17:234–257, 2008.
[62] R. Ober. Balanced parametrization of classes of linear systems. *SIAM J. Control Optim.*, 29:1251, 1991.
[63] A. Odabasioglu, M. Celik, and L. T. Pileggi. PRIMA: Passive reduced-order interconnect macromodeling algorithm. *IEEE Trans. Comput.-Aided Des. Integr. Circuits Syst.*, 17(8):645–654, 1998.
[64] P. C. Opdenacker and E. A. Jonckheere. A contraction mapping preserving balanced reduction scheme and its infinity norm error bounds. *IEEE Trans. Circuits Syst.*, 35(2):184–189, 1988.
[65] J. R. Phillips, L. Daniel, and L. M. Silveira. Guaranteed passive balancing transformations for model order reduction. *IEEE Trans. Comput.-Aided Des. Integr. Circuits Syst.*, 22(8):1027–1041, 2003.
[66] V.-M. Popov. Absolute stability of nonlinear systems of automatic control. *Autom. Remote Control*, 22(8):857–875, 1962.
[67] T. Reis. Circuit synthesis of passive descriptor systems: a modified nodal approach. *Int. J. Circuit Theory Appl.*, 38(1):44–68, 2010.
[68] T. Reis and T. Stykel. Positive real and bounded real balancing for model reduction of descriptor systems. *Int. J. Control*, 83(1):74–88, 2010.
[69] W. Rudin. *Real and Complex Analysis*, 3rd edition. McGraw-Hill, Inc., New York, NY, USA, 1987.
[70] E. R. Samuel, L. Knockaert, F. Ferranti, and T. Dhaene. Guaranteed passive parameterized macromodeling by using Sylvester state-space realizations. *IEEE Trans. Microw. Theory Tech.*, 61(4):1444–1454, 2013.
[71] D. Saraswat, R. Achar, and M. S. Nakhla. Global passivity enforcement algorithm for macromodels of interconnect subnetworks characterized by tabulated data. *IEEE Trans. Very Large Scale Integr. (VLSI) Syst.*, 13(7):819–832, 2005.
[72] D. Saraswat, R. Achar, and M. S. Nakhla. Fast passivity verification and enforcement via reciprocal systems for interconnects with large order macromodels. *IEEE Trans. Very Large Scale Integr. (VLSI) Syst.*, 15(1):48–59, 2007.
[73] C. S. Saunders, J. Hu, C. E. Christoffersen, and M. B. Steer. Inverse singular value method for enforcing passivity in reduced-order models of distributed structures for transient and steady-state simulation. *IEEE Trans. Microw. Theory Tech.*, 59(4):837–847, 2011.
[74] C. Scherer and S. Weiland. *Linear matrix inequalities in control. Lecture Notes*. Dutch Institute for Systems and Control, Delft, The Netherlands, 2000.
[75] A. Semlyen and B. Gustavsen. A half-size singularity test matrix for fast and reliable passivity assessment of rational models. *IEEE Trans. Power Deliv.*, 24(1):345–351, 2009.
[76] R. N. Shorten, P. Curran, K. Wulff, and E. Zeheb. A note on spectral conditions for positive realness of transfer function matrices. *IEEE Trans. Autom. Control*, 53(5):1258–1261, 2008.
[77] J. F. Sturm. Using SeDuMi 1.02, a Matlab toolbox for optimization over symmetric cones. *Optim. Methods Softw.*, 11(1–4):625–653, 1999.
[78] T. Stykel. Gramian-based model reduction for descriptor systems. *Math. Control Signals Syst.*, 16(4):297–319, 2004.
[79] F. Tisseur. A chart of backward errors for singly and doubly structured eigenvalue problems. *SIAM J. Matrix Anal. Appl.*, 24(3):877–897, 2003.
[80] P. Triverio, S. Grivet-Talocia, and M. S. Nakhla. A parameterized macromodeling strategy with uniform stability test. *IEEE Trans. Adv. Packaging*, 32(1):205–215, 2009.
[81] P. Triverio, S. Grivet-Talocia, M. S. Nakhla, F. Canavero, and R. Achar. Stability, causality, and passivity in electrical interconnect models. *IEEE Trans. Adv. Packaging*, 30(4):795–808, 2007.
[82] L. Vandenberghe and S. Boyd. Semidefinite programming. *SIAM Rev.*, 38(1):49–95, 1996.

[83] Y. Wang, Z. Zhang, C.-K. Koh, G. K.-H. Pang, and N. Wong PEDS. Passivity enforcement for descriptor systems via Hamiltonian-symplectic matrix pencil perturbation. In *Computer-Aided Design (ICCAD), 2010 IEEE/ACM International Conference on*, pages 800–807, 2010.

[84] Y. Wang, Z. Zhang, C.-K. Koh, G. Shi, G. K.-H. Pang, and N. Wong. Passivity enforcement for descriptor systems via matrix pencil perturbation. *IEEE Trans. Comput.-Aided Des. Integr. Circuits Syst.*, 31(4):532–545, 2012.

[85] D. S. Watkins. On Hamiltonian and symplectic Lanczos processes. *Linear Algebra Appl.*, 385(0):23–45, 2004. Special Issue in honor of Peter Lancaster.

[86] J. H. Wilkinson. *The algebraic eigenvalue problem*. Clarendon Press, 1965.

[87] J. C. Willems. Least squares stationary optimal control and the algebraic Riccati equation. *IEEE Trans. Autom. Control*, 16(6):621–634, 1971.

[88] J. C. Willems. Dissipative dynamical systems part I: General theory. *Arch. Ration. Mech. Anal.*, 45(5):321–351, 1972.

[89] J. C. Willems. Dissipative dynamical systems part II: Linear systems with quadratic supply rates. *Arch. Ration. Mech. Anal.*, 45(5):352–393, 1972.

[90] M. R. Wohlers. *Lumped and Distributed Passive Networks*. Academic press, 1969.

[91] N. Wong and C.-K. Chu. A fast passivity test for stable descriptor systems via skew-Hamiltonian/Hamiltonian matrix pencil transformations. *IEEE Trans. Circuits Syst. I, Regul. Pap.*, 55(2):635–643, 2008.

[92] V. A. Yakubovich. Solution of certain matrix inequalities encountered in non-linear control theory. In *Doklady Akademii Nauk*, volume 156, pages 278–281. Russian Academy of Sciences, 1964.

[93] Z. Ye, L. M. Silveira, and J. R. Phillips. Fast and reliable passivity assessment and enforcement with extended Hamiltonian pencil. In *Computer-Aided Design - Digest of Technical Papers, 2009. ICCAD 2009. IEEE/ACM International Conference on*, pages 774–778, 2009.

[94] Z. Ye, L. M. Silveira, and J. R. Phillips. Extended Hamiltonian pencil for passivity assessment and enforcement for S-parameter systems. In *Design, Automation Test in Europe Conference Exhibition (DATE), 2010*, pages 1148–1152, 2010.

[95] A. Zanco, S. Grivet-Talocia, T. Bradde, and M. De Stefano. Enforcing passivity of parameterized LTI macromodels via hamiltonian-driven multivariate adaptive sampling. *IEEE Trans. Comput.-Aided Des. Integr. Circuits Syst.*, 39(1):225–238, 2020.

[96] Z. Zhang and N. Wong. An efficient projector-based passivity test for descriptor systems. *IEEE Trans. Comput.-Aided Des. Integr. Circuits Syst.*, 29(8):1203–1214, 2010.

[97] Z. Zhang and N. Wong. Passivity check of S-parameter descriptor systems via S-parameter generalized Hamiltonian methods. *IEEE Trans. Adv. Packaging*, 33(4):1034–1042, 2010.

[98] Z. Zhang and N. Wong. Passivity test of immittance descriptor systems based on generalized Hamiltonian methods. *IEEE Trans. Circuits Syst. II, Express Briefs*, 57(1):61–65, 2010.

[99] K. Zhou, J. C. Doyle, and K. Glover. *Robust and optimal control*. Prentice Hall, Upper Saddle River, NJ, 1996.